On a chemotactic host-pathogen model: boundedness, aggregation, and segregation

Guodong Liu[a,b], Hao Wang[b,*], Xiaoyan Zhang[a]

[a] School of Mathematics, Shandong University, Jinan 250100, China

[b] Interdisciplinary Lab for Mathematical Ecology & Epidemiology,

Department of Mathematical and Statistical Sciences,

University of Alberta, Edmonton T6G 2G1, Canada

Abstract

This study formulates a host-pathogen model driven by cross-diffusion to examine the effect of chemotaxis on solution dynamics and spatial structures. The negative binomial incidence mechanism is incorporated to illustrate the transmission process by pathogens. In terms of the magnitude of chemotaxis, the global solvability of the model is extensively studied by employing semigroup methods, loop arguments, and energy estimates. In a limiting case, the necessary conditions for chemotaxis-driven instability are established regarding the degree of chemotactic attraction. Spatial aggregation may occur along strong chemotaxis in a two-dimensional domain due to solution explosion. We further observe that spatial segregation appears for short-lived free pathogens in a one-dimensional domain, whereas strong chemotactic repulsion homogenizes the infected hosts and thus fails to segregate host groups effectively.

Keywords: host-pathogen model; chemotaxis; boundedness; aggregation; segregation

MSC codes: 92D30; 92D50; 35B35; 35K57

*Corresponding author. Email: hao8@ualberta.ca

1 Introduction

Pathogenic organisms including viruses, bacteria, fungi, parasites, and helminths have significant effects on the dynamics of their host as demonstrated in a series of theoretical studies beginning with the work of Anderson and May [1–3]. Microbial pathogens continue to be a prominent etiological factor underlying infectious diseases affecting both humans and animals, as well as plants. In recent years, mathematical and computational approaches have effectively been employed to investigate host-pathogen models from several perspectives [4–8].

In [5], Dwyer proposed a host-pathogen model in a one-dimensional space to compare the spatial spread of the viruses Gilpinia hercyniae and Oryctes rhinoceros in the form of the following system of equations:

$$\begin{cases} \dfrac{dv_1}{dt} = r\left(1 - \dfrac{v_1+v_2}{K}\right)v_1 - \beta v_1 v_3 + D\dfrac{\partial^2 v_1}{\partial x^2}, \\ \dfrac{dv_2}{dt} = \beta v_1 v_3 - \left(\theta + r\dfrac{v_1+v_2}{K}\right)v_2 + D\dfrac{\partial^2 v_2}{\partial x^2}, \\ \dfrac{dv_3}{dt} = \gamma v_2 - \alpha v_3. \end{cases} \tag{1.1}$$

Here, $v_1 = v_1(x,t)$ and $v_2 = v_2(x,t)$ are the density of susceptible and infected hosts at position x and time t, respectively. $v_3 = v_3(x,t)$ is the concentration of the pathogen in an external environment at position x and time t. The underlying modelling assumptions are that (i) hosts move randomly with constant diffusion rate $D > 0$ while pathogens exhibit no capability for movement; (ii) hosts adhere to the principle of logistic growth with the intrinsic growth rate $r > 0$ and the carrying capacity $K > 0$; (iii) susceptible hosts can only be infected by pathogens obeying the mass-action law $\beta v_1 v_3$ with $\beta > 0$, and infected hosts reduce at the rate $\theta > 0$; (iv) pathogen particles are produced by v_2 at the rate $\gamma > 0$, and diminish at the rate $\alpha > 0$. We mention that model (1.1) includes the density-dependent host population dynamics due to the terms $-r\dfrac{v_1+v_2}{K}v_1$ and $-r\dfrac{v_1+v_2}{K}v_2$, which is a modification of Aderson and May's model in [3]. It is found in [5] that the introduction of host movement behavior also gives rise to the possibility of cycles of outbreaks in space and time simultaneously, illustrating the profound effect of spatial and temporal heterogeneity on population dynamics.

However, it is acknowledged that the mass-action law may not always be appropriate for describing the transmission processes of diverse infectious diseases. For example, it fails to incorporate the saturated effect of the population in certain scenarios. Therefore, the saturated incidence emerges as a more applicable mechanism to illustrate the transmission of diseases among hosts, which takes the following form [9, 10]:

$$f(v_1, v_2) = \frac{\beta v_1 v_2}{1 + \sigma v_2},$$

where $\sigma > 0$ is a positive constant used to measure the saturation degree, and $\delta > 0$ is the infection rate by infected hosts. It is clear that $f(v_1, v_2) \to \beta v_1 v_2$ as $\sigma \to 0$, and can be viewed as a generalized version of mass-action law. In [11], McCallum et al. investigated how to model pathogen transmission and outlined a negative binomial transmission mechanism between susceptible hosts and pathogen particles:

$$g(v_1, v_3) = k v_1 \ln\left(1 + \frac{\beta v_3}{k}\right).$$

Here $\beta > 0$ is the infection rate by pathogens, and the parameter $k > 0$ plays a critical role in this mechanism. The impact of this mechanism on disease transmission can vary depending on the values of k. As demonstrated in [11], small k corresponds to highly aggregated infection, while $g(v_1, v_3) \to \beta v_1 v_3$ as $k \to \infty$. In [12–14], the authors also studied this mechanism through numerical simulation. To the best of our knowledge, there are no existing efforts providing a robust theoretical analysis on the negative binomial transmission mechanism in host-pathogen models.

The cross-diffusion term $\chi \nabla \cdot (u \nabla v)$ is commonly applied to depict the phenomenon of chemotaxis [15, 16] between two different species or two biological groups u and v. It captures how the movement of one species is influenced by the concentration gradient of another species. Here, $\chi \in \mathbb{R}$ measures the magnitude of such effect. If $\chi < 0$, then u will be chemotactically attracted to v; while u will be chemotactically repulsed by v if $\chi > 0$.

The combination of chemotaxis and negative binomial transmission will pose a challenge to the problem. To simplify the analysis, we make a slight adjustment in the reaction term for susceptible hosts by replacing the logistic growth in system (1.1) with a simpler combination of recruitment and death rates. We now consider a reaction-chemotaxis-diffusion

host-pathogen model in a bounded domain $\Omega \subset \mathbb{R}^n (n \geq 1)$ with smooth boundary $\partial\Omega$, taking the following form:

$$\begin{cases} \partial_t v_1 - d_1 \Delta v_1 = \chi \nabla \cdot (v_1 \nabla v_2) + \Lambda(x) - \mu v_1 - \dfrac{\delta(x) v_1 v_2}{1+\sigma v_2} \\ \qquad\qquad - k v_1 \ln\left(1 + \dfrac{\beta(x) v_3}{k}\right), & x \in \Omega,\ t > 0, \\ \partial_t v_2 - d_2 \Delta v_2 = \dfrac{\delta(x) v_1 v_2}{1+\sigma v_2} + k v_1 \ln\left(1 + \dfrac{\beta(x) v_3}{k}\right) - \theta v_2, & x \in \Omega,\ t > 0, \\ \partial_t v_3 - d_3 \Delta v_3 = \gamma v_2 - \alpha v_3, & x \in \Omega,\ t > 0, \\ \nabla v_1 \cdot \mathbf{n} = \nabla v_2 \cdot \mathbf{n} = \nabla v_3 \cdot \mathbf{n} = 0, & x \in \partial\Omega,\ t > 0, \\ v_1(x,0) = v_{10}(x),\ v_2(x,0) = v_{20}(x),\ v_3(x,0) = v_{30}(x), & x \in \Omega. \end{cases} \tag{1.2}$$

Here, $\mathbf{n}$ represents the unit outward normal vector at $x \in \partial\Omega$. The distinct positive constants d_1, d_2, and d_3 are the respective diffusion rates of v_1, v_2, and v_3, where v_1, v_2, and v_3 have the same meanings as those in model (1.1). We apply the saturated incidence rate between v_1 and v_2, and the negative binomial transmission mechanism between v_1 and v_3. Taking spatial heterogeneity into consideration, the parameters $\Lambda(x)$, $\delta(x)$, and $\beta(x)$ exhibit spatial variation, where $\Lambda(x)$ is the recruitment rate of hosts, $\delta(x)$ is the infection rate by v_2, and $\beta(x)$ is the infection rate by v_3. μ and θ are positive constants, where μ measures the natural death rate of susceptible hosts, and θ denotes the death rate of infected hosts. The positive constant α means the death rate of pathogens in an external environment. Infected hosts can produce pathogens with the rate $\gamma > 0$. In model (1.2), we use the linear function $\Lambda(x) - \mu v_1$ to denote the external source (or supply) for susceptible hosts. One may refer to [17] and the reference therein. It is found in [17] that the external source can influence the dynamics of the population. We assume that susceptible hosts can only recognize the higher density of infected hosts by their symptoms of infection, while those are unable to perceive the higher concentration of pathogen particles because they are undetectable by ordinary observation. Homogeneous Neumann boundary conditions are applied to the system to represent the zero-flux across the boundary. In this paper, when χ is positive, the chemotaxis term indicates that susceptible hosts exhibit a behavioral tendency that they tend to move away from regions with a higher density of infected hosts. When χ is negative, the chemotaxis term may represent a case that in some special domains such as epidemic

areas or hospitals, susceptible hosts shall move to regions with a higher density of infected hosts. The chemotaxis effect disappears as χ tends to zero. Throughout the whole paper, we make the following assumption:

(H1) Parameters $\Lambda(x)$, $\delta(x)$, and $\beta(x)$ are positive Hölder continuous functions on $\bar{\Omega}$.

(H2) The initial data $v_{10}(x)$, $v_{20}(x)$, and $v_{30}(x)$ are nonnegative. In addition, $\int_\Omega [v_{20}(x) + v_{30}(x)]dx > 0$.

The cross-diffusion $\chi\nabla \cdot (v_1 \nabla v_2)$ serves as a mechanism employed by susceptible hosts either to avoid infection by staying away from infected hosts (known as the repulsive chemotaxis phenomenon), or to approach infected hosts for providing treatment (known as the attractive chemotaxis phenomenon). The chemotaxis term has been widely shown to exert a strong effect in driving solutions of the underlying models to blow up in finite or infinite time, as can be seen in the extensively studied Keller-Segel chemotaxis systems [18,19]. Therefore, the global solvability of model (1.2) is an important consideration. Horstmann and Winkler investigated the boundedness and blow-up of the solution in a chemotaxis system, and they determined the critical blow-up exponent for a Keller-Segel type model in [20]. In [21], Li et al. applied the chemotaxis term to a reaction-diffusion susceptible-infected-susceptible model with a frequency-dependent incidence mechanism. With the key observation that the solution of the infected component is always bounded, they established the global existence and boundedness of the classical solution. In [22], Bellomo et al. applied the chemotaxis term to a May-Nowak model, where they used loop arguments to get the global boundedness of the solution for the weak chemotaxis effect. Most recently, Li and Xiang made use of a series of energy estimates to obtain the boundedness of an epidemic model with the chemotaxis term and power-like incidence mechanism by imposing restrictions on the magnitude of the chemotaxis and the power of the incidence in [23].

The spatial heterogeneity of environments and mutual interactions of individuals may result in different spatial structures [24], including aggregation and segregation. Spatial aggregation is a pattern where the species exhibit significant concentration at specific positions. Spatial segregation is a phenomenon where two similar species segregate each other in their habitat [25]. We are interested in whether the chemotactic host-pathogen model allows for the formation of spatial structures.

The rest of the work is organized as follows. In section 2, we investigate the global existence and boundedness of the solution to model (1.2) in three cases: zero χ, small χ, and arbitrary χ (including large χ). In section 3, threshold dynamics are established in terms of the basic reproduction number. Additionally, under the chemotactic attraction, the chemotaxis-driven instability of a limiting case as $\sigma \to 0$ and $k \to \infty$ is explored. In section 4, we present a series of numerical simulations to verify the global existence and boundedness of the solution in one- and two-dimensional domains. Spatial aggregation and segregation phenomena are illustrated with respect to varying values of χ. The analytical and numerical results are summarized in the final section.

2 Boundedness of the global solution

We consider the global solvability and boundedness of the solution to (1.2) regarding the magnitude of the chemotaxis effect. It includes three cases in this section: zero χ, small χ, and arbitrary χ. For notational convenience, we use $\|\cdot\|_q$ to represent the norm $\|\cdot\|_{L^q(\Omega)}$ of $L^q(\Omega)$ for $q > 0$. Denote $u^* := \max_{x\in\bar{\Omega}} u(x)$, where $u(x)$ can be taken as $\Lambda(x)$, $\delta(x)$, and $\beta(x)$. Let $|\Omega|$ denote the volume of Ω.

For any χ, it is not difficult to obtain L^1-estimates for the solution.

Lemma 2.1. *Assume $(v_{10}, v_{20}, v_{30}) \in C(\bar{\Omega}, \mathbb{R}^3_+)$. The following L^1-estimates hold.*

$$\begin{aligned}\int_\Omega v_1 dx,\ \int_\Omega v_2 dx,\ \int_\Omega v_3 dx &\le \max\left\{1, \frac{\gamma}{\alpha}\right\}\left(\int_\Omega (v_{10}+v_{20})dx + \frac{\Lambda^*|\Omega|}{\min\{\mu,\theta\}}\right) + \int_\Omega v_{30}dx \\ &=: M_1,\ \forall\ t \ge 0. \end{aligned} \tag{2.1}$$

$$\limsup_{t\to\infty}\int_\Omega v_1 dx,\ \limsup_{t\to\infty}\int_\Omega v_2 dx,\ \limsup_{t\to\infty}\int_\Omega v_3 dx \le \max\left\{1, \frac{\gamma}{\alpha}\right\}\frac{\Lambda^*|\Omega|}{\min\{\mu,\theta\}} =: N_1. \tag{2.2}$$

Proof. It follows from the maximum principle that the solution (v_1, v_2, v_3) of model (1.2) is nonnegative. Adding the first two equations of (1.2) and integrating the result over Ω by parts lead to

$$\frac{d}{dt}\int_\Omega (v_1+v_2)dx = \int_\Omega \Lambda(x)dx - \int_\Omega(\mu v_1 + \theta v_2)dx \le \Lambda^*|\Omega| - a\int_\Omega (v_1+v_2)dx,\ \forall\ t > 0.$$

where $a = \min\{\mu, \theta\}$. Then Gronwall's inequality says that

$$\int_\Omega (v_1 + v_2)dx \le e^{-at} \int_\Omega (v_{10} + v_{20})dx + \frac{\Lambda^*|\Omega|}{a}(1 - e^{-at}),\ \forall\ t > 0. \tag{2.3}$$

Integrating the third equation of (1.2) over Ω by part gives

$$\frac{d}{dt}\int_\Omega v_3 dx \le \gamma \int_\Omega v_2 dx - \alpha \int_\Omega v_3 dx,\ \forall\ t > 0.$$

Applying Gronwall's inequality again, we have

$$\int_\Omega v_3 dx \le e^{-\alpha t} \int_\Omega v_{30} dx + \frac{\gamma \int_\Omega v_2 dx}{\alpha}(1 - e^{-\alpha t}),\ \forall\ t > 0. \tag{2.4}$$

Combining (2.3) and (2.4), we readily obtain (2.1) and (2.2). □

2.1 The case of zero χ

When $\chi = 0$, model (1.2) decays to a standard reaction-diffusion system. With reference to the standard theory for parabolic equations in [26], we give the following lemma on the local existence and finite-time blow-up of the classical solution to (1.2).

Lemma 2.2. *For any $(v_{10}, v_{20}, v_{30}) \in C(\bar{\Omega}, \mathbb{R}^3_+)$, model (1.2) admits a unique nonnegative classical solution $(v_1(\cdot,t), v_2(\cdot,t), v_3(\cdot,t))$ defined on $\bar{\Omega} \times [0, T_{\max})$ with $T_{\max} \le \infty$. Moreover, if $T_{\max} < \infty$, then*

$$\lim_{t \to T^-_{\max}} (\|v_1(\cdot,t)\|_\infty + \|v_2(\cdot,t)\|_\infty + \|v_3(\cdot,t)\|_\infty) = \infty.$$

Theorem 2.1. *For any $(v_{10}, v_{20}, v_{30}) \in C(\bar{\Omega}, \mathbb{R}^3_+)$, model (1.2) admits a unique nonnegative classical solution $(v_1(\cdot,t), v_2(\cdot,t), v_3(\cdot,t))$ defined on $\bar{\Omega} \times [0, \infty)$.*

Proof. The uniqueness and nonnegativity of the local solution to (1.2) are demonstrated by Lemma 2.2. It suffices to verify the global existence of the solution. For $i = 1, 2, 3$, let $T_i(t)$ be the semigroup generated by the operator $\mathcal{A}_i$ in $C(\bar{\Omega})$ with Neumann boundary condition, where $\mathcal{A}_1 = d_1\Delta - \mu$, $\mathcal{A}_2 = d_2\Delta - \theta$, and $\mathcal{A}_3 = d_3\Delta - \alpha$. It is well-known that $\|T_i(t)\|_\infty \le e^{-\lambda_i t}$, where $\lambda_i > 0$ is the principal eigenvalue of $-\mathcal{A}_i$ with Neumann boundary condition for $i = 1, 2, 3$. In view of the first equation of (1.2), we see that

$$v_1(\cdot,t) \le T_1(t)v_{10} + \int_0^t T_1(t-s)\Lambda(\cdot)ds,\ \forall\ t \in [0, T_{\max}).$$

This results in

$$\begin{aligned}\|v_1(\cdot,t)\|_\infty &\le \|T_1(t)\|_\infty\|v_{10}\|_\infty + \Lambda^*\int_0^t \|T_1(t-s)\|_\infty ds\\ &\le e^{-\lambda_1 t}\|v_{10}\|_\infty + \frac{\Lambda^*}{\lambda_1}(1-e^{-\lambda_1 t})\\ &\le \|v_{10}\|_\infty + \frac{\Lambda^*}{\lambda_1} =: K_1,\ \forall\ t\in[0,T_{\max}). \end{aligned} \tag{2.5}$$

It follows from the second equation of (1.2) that

$$\begin{aligned}v_2(\cdot,t) &= T_2(t)v_{20} + \int_0^t T_2(t-s)\bigg(\frac{\delta v_1(\cdot,t)v_2(\cdot,t)}{1+\sigma v_2(\cdot,t)}\\ &\quad + kv_1(\cdot,t)\ln\left(1+\frac{\beta v_3(\cdot,t)}{k}\right)\bigg)ds,\ \forall\ t\in[0,T_{\max}).\end{aligned}$$

Consequently, by virtue of $\ln(1+u)\le u$ for $u\ge 0$ and (2.5), we have for all $t\in[0,T_{\max})$,

$$\begin{aligned}\|v_2(\cdot,t)\|_\infty &\le e^{-\lambda_2 t}\|v_{20}\|_\infty + \int_0^t e^{-\lambda_2(t-s)}(\delta^*/\sigma\|v_1\|_\infty + \beta^*\|v_1(\cdot,s)\|_\infty\|v_3(\cdot,s)\|_\infty)ds\\ &\le e^{-\lambda_2 t}\|v_{20}\|_\infty + \frac{\delta^* K_1}{\sigma\lambda_2} + \beta^* K_1\int_0^t e^{-\lambda_2(t-s)}\|v_3(\cdot,s)\|_\infty ds. \end{aligned} \tag{2.6}$$

In a similar manner, we obtain

$$\|v_3(\cdot,t)\|_\infty \le e^{-\lambda_3 t}\|v_{30}\|_\infty + \gamma\int_0^t e^{-\lambda_3(t-s)}\|v_2(\cdot,s)\|_\infty ds,\ \forall\ t\in[0,T_{\max}). \tag{2.7}$$

Taking $0<\lambda_m<\min\{\frac{\lambda_2}{2},\lambda_3\}$ and substituting (2.7) into (2.6) produce

$$\begin{aligned}\|v_2(\cdot,t)\|_\infty &\le e^{-\lambda_2 t}\|v_{20}\|_\infty + \frac{K_1(\delta^*/\sigma+\beta^*\|v_{30}\|_\infty)}{\lambda_2}\\ &\quad + \beta^*\gamma K_1\int_0^t e^{-\lambda_2(t-s)}\int_0^s e^{-\lambda_3(s-\tau)}\|v_2(\cdot,\tau)\|_\infty d\tau ds\\ &\le \|v_{20}\|_\infty + \frac{K_1(\delta^*/\sigma+\beta^*\|v_{30}\|_\infty)}{\lambda_2}\\ &\quad + \beta^*\gamma K_1 e^{-\lambda_2 t}\int_0^t e^{\lambda_m\tau}\|v_2(\cdot,\tau)\|_\infty d\tau\int_\tau^t e^{(\lambda_2-\lambda_m)s}ds\\ &\le \|v_{20}\|_\infty + \frac{K_1(\delta^*/\sigma+\beta^*\|v_{30}\|_\infty)}{\lambda_2}\\ &\quad + \frac{\beta^*\gamma K_1 e^{-\lambda_m t}}{\lambda_2-\lambda_m}\int_0^t e^{\lambda_m\tau}\|v_2(\cdot,\tau)\|_\infty d\tau,\ \forall\ t\in[0,T_{\max}). \end{aligned} \tag{2.8}$$

Then by Gronwall's inequality, if $T_{\max}<\infty$, we can calculate

$$\|v_2(\cdot,t)\|_\infty \le a_1 e^{a_2 T_{\max}} =: K_2,\ \forall\ t\in[0,T_{\max}), \tag{2.9}$$

with $a_1 = \|v_{20}\|_\infty + \frac{K_1(\delta^*/\sigma+\beta^*\|v_{30}\|_\infty)}{\lambda_2}$ and $a_2 = \frac{\beta^*\gamma K_1}{\lambda_2-\lambda_m}$. By (2.7) and (2.9), we get

$$\|v_3(\cdot,t)\|_\infty \le \|v_{30}\|_\infty + \frac{\gamma K_2}{\lambda_3},\ \forall\ t \in [0, T_{\max}). \tag{2.10}$$

According to (2.5), (2.9), (2.10), and Lemma 2.2, we know $T_{\max} = \infty$ as desired. □

We now turn to derive the ultimate boundedness of the solution independent of the initial data. To this end, the following L^p-estimates independent of the initial data for the solution are necessary.

Lemma 2.3. *For any $p \ge 1$, there exists a positive constant N_p independent of the initial data such that*

$$\limsup_{t\to\infty}(\|v_2(\cdot,t)\|_p^p + \|v_3(\cdot,t)\|_p^p) \le N_p.$$

Proof. We first give the ultimate boundedness of $v_1(x,t)$ for t large enough. It follows from the first equation of (1.2) that

$$\partial_t v_1 \le d_1\Delta v_1 + \Lambda^* - \mu v_1.$$

By the standard comparison principle and Lemma 1 in [27], we infer that

$$\limsup_{t\to\infty} v_1(x,t) \le \lim_{t\to\infty} \bar{v}_1(x,t) = \frac{\Lambda^*}{\mu} =: \tilde{N},\ \text{uniformly for } x \in \bar{\Omega},$$

where $\bar{v}_1$ is the solution of

$$\begin{cases} \partial_t \bar{v}_1 - d_1\Delta\bar{v}_1 = \Lambda^* - \mu_*\bar{v}_1, & x \in \Omega,\ t > 0,\\ \nabla\bar{v}_1\cdot\mathbf{n} = 0, & x \in \partial\Omega,\ t > 0,\\ \bar{v}_1(x,0) = \bar{v}_{10}(x), & x \in \Omega. \end{cases}$$

This implies

$$\limsup_{t\to\infty}\|v_1(\cdot,t)\|_\infty \le \tilde{N}. \tag{2.11}$$

We then prove the following claim.

Claim. For any $m \ge 0$, there exists a positive constant N_{2^m} independent of the initial data such that

$$\limsup_{t\to\infty}(\|v_2(\cdot,t)\|_{2^m}^{2^m} + \|v_3(\cdot,t)\|_{2^m}^{2^m}) \le N_{2^m}. \tag{2.12}$$

We employ the induction method to prove this claim. It follows from (2.2) in Lemma 2.1 that (2.12) holds in the case of $m = 0$. Suppose that (2.12) holds for $m-1$ ($m > 1$), i.e., there exists a positive constant $N_{2^{m-1}}$ independent of the initial data such that

$$\limsup_{t\to\infty}(\|v_2(\cdot,t)\|_{2^{m-1}}^{2^{m-1}} + \|v_3(\cdot,t)\|_{2^{m-1}}^{2^{m-1}}) \le N_{2^{m-1}}. \tag{2.13}$$

Multiplying both sides of the second equation of (1.2) by $v_2^{2^{m-1}}$, and integrating over Ω by parts, then according to (2.11), we obtain that there exists $T_0 > 0$ such that

$$\begin{aligned}\frac{1}{2^m}\frac{d}{dt}\int_\Omega v_2^{2^m}dx \;\le\; & -\frac{d_2(2^m-1)}{2^{2m-2}}\int_\Omega |\nabla v_2^{2^{m-1}}|^2dx + \delta^*\tilde{N}\int_\Omega v_2^{2^m}dx + \delta^*\tilde{N} \\ & +\beta^*\tilde{N}\int_\Omega v_2^{2^m-1}v_3dx - \theta\int_\Omega v_2^{2^m}dx,\ \forall\ t \ge T_0. \end{aligned}\tag{2.14}$$

It follows from Young's inequality with epsilon that

$$\int_\Omega v_2^{2^m-1}v_3dx \le \epsilon_1\int_\Omega v_3^{2^m}dx + A_{\epsilon_1}\int_\Omega v_2^{2^m}dx, \tag{2.15}$$

where $\epsilon_1 = \frac{\alpha}{\beta^*\tilde{N}+\gamma}$ and A_{ϵ_1} is a positive constant depending on ϵ_1.

We multiply both sides of the third equation of (1.2) by $v_3^{2^{m-1}}$ and integrate over Ω by parts to find

$$\begin{aligned}\frac{1}{2^m}\frac{d}{dt}\int_\Omega v_3^{2^m}dx \;\le\; & -\frac{d_3(2^m-1)}{2^{2m-2}}\int_\Omega |\nabla v_3^{2^{m-1}}|^2dx + \gamma\int_\Omega v_2v_3^{2^m-1}dx \\ & -\alpha\int_\Omega v_3^{2^m}dx,\ \forall\ t \ge T_0. \end{aligned}\tag{2.16}$$

It follows from Young's inequality with epsilon again that

$$\int_\Omega v_2v_3^{2^m-1}dx \le \epsilon_2\int_\Omega v_3^{2^m}dx + A_{\epsilon_2}\int_\Omega v_2^{2^m}dx, \tag{2.17}$$

where $\epsilon_2 = \epsilon_1$ and A_{ϵ_2} is a positive constant depending on ϵ_2.

Recall the following interpolation inequality: for any $\epsilon > 0$, there exists $C_\epsilon > 0$ depending on ϵ such that

$$\|u\|_2^2 \le \epsilon\|\nabla u\|_2^2 + C_\epsilon\|u\|_1^2 \text{ for any } u \in H^1(\Omega). \tag{2.18}$$

Applying (2.18) with $\epsilon_3 = \frac{d_3(2^m-1)}{2^{2m-2}}$ to the first term of the right-hand side of (2.16), we get

$$-\epsilon_3\int_\Omega |\nabla v_3^{2^{m-1}}|^2dx \le -\int_\Omega v_3^{2^m}dx + A_{\epsilon_3}\left(\int_\Omega v_3^{2^{m-1}}dx\right)^2. \tag{2.19}$$

We apply (2.18) again with $\epsilon_4 = \frac{d_2(2^m-1)}{2^{2m-2}(\delta^*\tilde{N}+\beta^*\tilde{N}A_{\epsilon_1}+\gamma A_{\epsilon_2}+1)}$ to the first term of the right-hand side of (2.14) to estimate

$$-\epsilon_4 \int_\Omega |\nabla v_2^{2^{m-1}}|^2 dx \le -\int_\Omega v_2^{2^m} dx + A_{\epsilon_4} \left(\int_\Omega v_2^{2^{m-1}} dx \right)^2. \tag{2.20}$$

Therefore, according to (2.14)-(2.17), (2.19), and (2.20), one has

$$\begin{aligned} \frac{1}{2^m}\frac{d}{dt}\int_\Omega (v_2^{2^m}+v_3^{2^m})dx \;\; &\le \;\; -\int_\Omega (v_2^{2^m}+v_3^{2^m})dx + A_{\epsilon_3}\left(\int_\Omega v_3^{2^{m-1}}dx\right)^2 + \delta^*\tilde{N} \\ &\quad +(\delta^*\tilde{N}+\beta^*\tilde{N}A_{\epsilon_1}+\gamma A_{\epsilon_2}+1)A_{\epsilon_4}\left(\int_\Omega v_2^{2^{m-1}}dx\right)^2, \;\forall\; t \ge T_0. \end{aligned}$$

Then by (2.13), Gronwall's inequality entails

$$\limsup_{t\to\infty}(\|v_2(\cdot,t)\|_{2^m}^{2^m}+\|v_3(\cdot,t)\|_{2^m}^{2^m}) \le \sqrt[2^m]{\delta^*\tilde{N}+(A_{\epsilon_3}+(\delta^*\tilde{N}+A_{\epsilon_1}+A_{\epsilon_2}+1)A_{\epsilon_4})N_{2^{m-1}}} =: N_{2^m},$$

and thereby completes the proof of the claim. With aid of the continuous embedding $L^q(\Omega) \subset L^p(\Omega)$ for $q \ge p \ge 1$, the assertion of Lemma 2.3 holds. □

By a standard analytical semigroup method, we can obtain the ultimate boundedness of the solution, which implies the existence of a global attractor for (1.2).

Theorem 2.2. *There exists a positive constant N_∞ independent of the initial data such that the solution of (1.2) satisfies*

$$\lim_{t\to\infty}(\|v_1(\cdot,t)\|_\infty + \|v_2(\cdot,t)\|_\infty + \|v_3(\cdot,t)\|_\infty) \le N_\infty. \tag{2.21}$$

Moreover, there exists a connected global attractor in $C(\bar{\Omega}, \mathbb{R}^3_+)$.

Proof. The ultimate boundedness of $v_1(x,t)$ is given in (2.11). To derive the ultimate boundedness of $v_2(x,t)$ and $v_3(x,t)$ for $x \in \Omega$ and t large enough, we employ the results of fractional power space. Let $J_2(t)$ be the analytic semigroup generated by $\mathcal{A}_2$ in $L^p(\Omega)$ with $D(\mathcal{A}_2) = \{u \in W^{2,p}(\Omega) : \; \nabla u \cdot \mathbf{n} = 0 \text{ on } \partial\Omega\}$, and $\mathbb{X}_{\alpha'},\ 0 \le \alpha' \le 1$ denote the fractional power space with graph norm. Pick $p > \frac{n}{2}$ and $\alpha' \ge \frac{n}{2p}$ such that $\mathbb{X}_{\alpha'} \subset L^\infty(\Omega)$. It follows from [28] that there exists $N_{\alpha'} > 0$ such that $\|A_2^{\alpha'} J_2(t)\| \le \frac{N_{\alpha'}}{t^{\alpha'}}$ for all $t > 0$. Using (2.11) and Lemma 2.3, there exists $T_\infty > 1$ such that

$$\|v_1(\cdot,t)\|_\infty \le \tilde{N} \text{ and } \|v_2(\cdot,t)\|_p, \|v_3(\cdot,t)\|_p \le N_p^{\frac{1}{p}}, \;\forall\; t \ge T_\infty. \tag{2.22}$$

In view of the second equation of (1.2), we know

$$v_2(t) \le J_2(t)v_2(\cdot,t-1) + \int_{t-1}^{t} J_2(t-s)(\delta v_1(\cdot,s)v_2(\cdot,s) + \beta v_1(\cdot,s)v_3(\cdot,s))ds,\ \forall\ t \ge T_\infty + 1.$$

By virtue of (2.22), we then calculate

$$\begin{aligned}
\|\mathcal{A}_2^{\alpha'} v_2(\cdot,t)\|_p &\le \|\mathcal{A}_2^{\alpha'} J_2(t)v_2(\cdot,t-1)\|_p \\
&\quad + \max\{\delta^*,\beta^*\}\tilde{N}\int_{t-1}^{t} \|\mathcal{A}_2^{\alpha'} J_2(t-s)(v_2(\cdot,s)+v_3(\cdot,s))\|_p ds \\
&\le N_{\alpha'} N_p^{\frac{1}{p}} + 2\max\{\delta^*,\beta^*\}\tilde{N} N_p^{\frac{1}{p}} \int_{t}^{t-1} \frac{N_{\alpha'}}{(t-s)^{\alpha'}} ds \\
&\le N_{\alpha'} N_p^{\frac{1}{p}} (1 + 2\max\{\delta^*,\beta^*\}\tilde{N}(1-\alpha')^{-1}),\ \forall\ t \ge T_\infty + 1. \qquad (2.23)
\end{aligned}$$

In a same manner, let $J_3(t)$ be the analytic semigroup generated by $\mathcal{A}_3$ in $L^p(\Omega)$ with $D(\mathcal{A}_3) = D(\mathcal{A}_2)$. We also have

$$\begin{aligned}
\|\mathcal{A}_3^{\alpha'} v_3(\cdot,t)\|_p &\le \|A_3^{\alpha'} J_3(t)v_3(\cdot,t-1)\|_p + \gamma\int_{t-1}^{t} \|\mathcal{A}_3^{\alpha'} J_3(t-s)v_2(\cdot,s)\|_p ds \\
&\le N_{\alpha'} N_p^{\frac{1}{p}} (1 + \gamma(1-\alpha')^{-1}),\ \text{for } t \ge T_\infty + 1. \qquad (2.24)
\end{aligned}$$

Then by (2.23), (2.24), and the continuous embedding $\mathbb{X}_{\alpha'} \subset L^\infty(\Omega)$, we get the ultimate boundedness of v_2 and v_3. This shows that (2.21) is valid.

Let $\Phi(t) : C(\bar{\Omega},\mathbb{R}^3_+) \to C(\bar{\Omega},\mathbb{R}^3_+),\ t \ge 0$ be the semigroup generated by the solution of (1.2). Then (2.21) implies that $\Phi(t)$ is point dissipative. Furthermore, $\Phi(t)$ is asymptotically smooth. Then by Theorem 3.4.8 in [29], we obtain the existence of a connected global attractor. □

2.2 The case of small χ

In this subsection, we study the boundedness of the solution when the chemotaxis is relatively mild. We use the Neumann heat semigroup method to state some estimates. The following lemma on the Neumann heat semigroup can be found from Lemma 1.3 in [30].

Lemma 2.4. *For $d > 0$, let $(e^{td\Delta})_{t\ge 0}$ be the Neumann heat semigroup and $\lambda_0 > 0$ be the principal eigenvalue of $-d\Delta$ on Ω. Then there exist some positive constants $k_i (i = 1,2,3,4)$ depending on d and Ω such that the following smoothing L^p-L^q type estimates hold:*

(i) If $1 \le q \le p \le \infty$, then for any $u \in L^q(\Omega)$,

$$\|e^{td\Delta}u\|_p \le k_1 \left(1 + t^{-\frac{n}{2}(\frac{1}{q}-\frac{1}{p})}\right) \|u\|_q, \ \forall\ t > 0.$$

(ii) If $1 \le q \le p \le \infty$, then for any $u \in L^q(\Omega)$,

$$\|\nabla e^{td\Delta}u\|_p \le k_2 \left(1 + t^{-\frac{1}{2}-\frac{n}{2}(\frac{1}{q}-\frac{1}{p})}\right) e^{-\lambda_0 t}\|u\|_q, \ \forall t > 0.$$

(iii) If $2 \le q \le p < \infty$, then for any $u \in W^{1,q}(\Omega)$,

$$\|\nabla e^{td\Delta}u\|_p \le k_3 \left(1 + t^{-\frac{n}{2}(\frac{1}{q}-\frac{1}{p})}\right) e^{-\lambda_0 t}\|\nabla u\|_q, \ \forall\ t > 0.$$

(iv) If $1 < q \le p \le \infty$, then for any $u \in (L^q(\Omega))^n$ and $u \cdot \mathbf{n} = 0$ on $\partial\Omega$,

$$\|e^{td\Delta}\nabla \cdot u\|_p \le k_4 \left(1 + t^{-\frac{1}{2}-\frac{n}{2}(\frac{1}{q}-\frac{1}{p})}\right) e^{-\lambda_0 t}\|u\|_q, \ \forall\ t > 0.$$

Similar to the proof of Theorem 3.1 in [20], we can obtain the following lemma on the local existence and finite-time blow-up of the solution to the reaction-chemotaxis-diffusion system.

Lemma 2.5. *Assume $v_{10}, v_{30} \in C(\bar{\Omega})$ and $v_{20} \in W^{1,q}(\Omega)$ for $q > n$. There exists a unique nonnegative solution $(v_1(\cdot,t), v_2(\cdot,t), v_3(\cdot,t))$ of (1.2) defined on $[0, T_{\max})$ with $T_{\max} \le \infty$ such that*

$$v_1, v_3 \in C(\bar{\Omega}\times[0,T_{\max}))\cap C^{2,1}(\bar{\Omega}\times(0,T_{\max})) \text{ and } v_2 \in C([0,T_{\max}); W^{1,q}(\Omega))\cap C^{2,1}(\bar{\Omega}\times(0,T_{\max})).$$

Moreover, if $T_{\max} < \infty$, then

$$\lim_{t\to T_{\max}^-} (\|v_1(\cdot,t)\|_\infty + \|v_2(\cdot,t)\|_{W^{1,q}(\Omega)} + \|v_3(\cdot,t)\|_\infty) = \infty.$$

Now, we use the loop arguments in [22] to bootstrap the boundedness of the solution. The following auxiliary lemmas assert that we can achieve some estimates for v_1, ∇v_2, and v_3 depending on the bounds for v_1 and v_3 as assumed for a local time interval.

Lemma 2.6. *Assume $v_{10}, v_{30} \in C(\bar{\Omega})$ and $v_{20} \in W^{1,q}(\Omega)$ for $q > n$. Given $T^* \in (0, T_{\max})$, assume there exist positive constants L_1 and L_3 depending on T such that*

$$\|v_1(\cdot,t)\|_\infty \le L_1, \ \|v_3(\cdot,t)\|_\infty \le L_3, \ \forall\ t \in (0,T^*). \tag{2.25}$$

Then there exist positive constants B_1, B_2 and B_3 independent of L_1 and L_3 such that

$$\|\nabla v_2(\cdot,t)\|_q \le B_1 + B_2 L_1 + B_3 L_1 L_3^\rho$$

for $\rho := \frac{q-1}{q} \in (0,1)$.

Proof. According to the second equation of (1.2), we derive

$$v_2(\cdot,t) = e^{t(d_2\Delta-\theta)}v_{20} + \int_0^t e^{(t-s)(d_2\Delta-\theta)}\left(\frac{\delta^*}{\sigma}v_1(\cdot,s) + \beta^* v_1(\cdot,s)v_3(\cdot,s)\right)ds,\ \forall\ t\in(0,T^*).$$

Further, by (ii) and (iii) in Lemma 2.4, one has

$$\begin{aligned}\|\nabla v_2(\cdot,t)\|_q &\le \|\nabla e^{t(d_2\Delta-\theta)}v_{20}\|_q + \int_0^t \left\|\nabla e^{(t-s)(d_2\Delta-\theta)}\left(\frac{\delta^*}{\sigma}v_1(\cdot,s) + \beta^* v_1(\cdot,s)v_3(\cdot,s)\right)\right\|_q ds\\ &\le k_3\|v_{20}\|_{W^{1,q}} + \frac{\delta^* k_2}{\sigma}\int_0^t e^{-(t-s)\theta}(1+(t-s)^{-\frac{1}{2}})\|v_1(\cdot,s)\|_q ds\\ &\quad +\beta^* k_2\int_0^t e^{-(t-s)\theta}(1+(t-s)^{-\frac{1}{2}})\|v_1(\cdot,s)v_3(\cdot,s)\|_q ds,\ \forall\ t\in(0,T^*). \quad (2.26)\end{aligned}$$

An application of Hölder's inequality gives

$$\begin{aligned}\|v_1(\cdot,s)v_3(\cdot,s)\|_q &\le \|v_1(\cdot,s)\|_\infty\|v_3(\cdot,s)\|_q\\ &\le \|v_1(\cdot,s)\|_\infty\|v_3(\cdot,s)\|_\infty^\rho\|v_3(\cdot,s)\|_1^{1-\rho},\ \forall s\in(0,T^*). \quad (2.27)\end{aligned}$$

Note that (2.1) is also valid for $v_{20}\in W^{1,q}(\Omega)$. Then by means of (2.1) and (2.25), inserting (2.27) to (2.26) produces

$$\|\nabla v_2(\cdot,t)\|_q \le k_3\|v_{20}\|_{W^{1,q}} + \frac{\delta^* k_2 b_1}{\sigma}L_1 + \beta^* k_2 b_1 M_1^{1-\rho}L_1 L_3^\rho,\ \forall\ t\in(0,T^*),$$

where $b_1 := \int_0^\infty (1+s^{-\frac{1}{2}})e^{-d_2 s}ds$. This completes the proof with

$$B_1 := k_3\|v_{20}\|_{W^{1,q}},\ B_2 := \frac{\delta^* k_2 b_1}{\sigma} \text{ and } B_3 := \beta^* k_2 b_1 M_1^{1-\rho}.$$

□

Lemma 2.7. *Assume $v_{10}, v_{30}\in C(\bar\Omega)$ and $v_{20}\in W^{1,q}(\Omega)$ for $q>n$. Given $T^*\in(0,T_{\max})$, assume (2.25) still holds. Then there exists B_4 independent of L_1 and L_3 such that*

$$\|v_3(\cdot,t)\|_\infty \le B_4(1+L_1+L_1L_3^\rho),\ \forall\ t\in(0,T^*), \quad (2.28)$$

where $\rho\in(0,1)$ is as in Lemma 2.6.

Proof. As $q > n$, we have $W^{1,q}(\Omega) \subset L^\infty(\Omega)$. Then by Poincaré's inequality, we know that there exists some positive constant C such that

$$\|u\|_\infty \le C\|u\|_{W^{1,q}(\Omega)} \le C(\|\nabla u\|_q + \|u\|_{p'}), \tag{2.29}$$

for any $p' \ge 1$. Note that (2.1) is still valid for $v_{20} \in W^{1,q}(\Omega),\ q > n$. By Lemma 2.6 and (2.1), we now choose $p' = 1$ in (2.29), and hence

$$\|v_2(\cdot,t)\|_\infty \le C(B_1 + B_2L_1 + B_3L_1L_3^\rho) + CM_1,\ \forall\ t \in (0,T^*). \tag{2.30}$$

Set $\bar v_3(x,t) := \max\left\{\|v_{30}\|_\infty, \max\left\{1, \frac{\gamma}{\alpha}\right\}[C(B_1 + B_2L_1 + B_3L_1L_3^\rho) + CM_1]\right\}$ for $(x,t) \in \bar\Omega \times [0,T^*)$. In view of (2.30), we then have

$$\begin{cases} \partial_t \bar v_3 - d_3\Delta \bar v_3 + \alpha \bar v_3 - \gamma v_2 = \alpha \bar v_3 - \gamma v_2 & \\ \ge 0 = \partial_t v_3 - d_3\Delta v_3 + \alpha v_3 - \gamma v_2, & (x,t) \in \Omega \times (0,T^*), \\ \nabla \bar v_3 \cdot \mathbf{n} = \nabla v_3 \cdot \mathbf{n} = 0, & (x,t) \in \partial\Omega \times (0,T^*), \\ \bar v_3(x,0) \ge \|v_{30}\|_\infty \ge v_{30}, & x \in \Omega. \end{cases}$$

The standard comparison principle enables us to derive $v_3 \le \bar v_3$ in $\Omega \times (0,T^*)$. Thus, (2.28) holds with

$$B_4 := \max\left\{\|v_{30}\|_\infty, C(B_1 + M_1)\max\left\{1, \frac{\gamma}{\alpha}\right\}, B_2\max\left\{1, \frac{\gamma}{\alpha}\right\}, B_3\max\left\{1, \frac{\gamma}{\alpha}\right\}\right\}.$$

□

Lemma 2.8. *Assume $v_{10}, v_{30} \in C(\bar\Omega)$ and $v_{20} \in W^{1,q}(\Omega)$ for $q > n$. Given $T^* \in (0, T_{\max})$, assume (2.25) holds with $L_3 \ge 1$. Then there exists B_5 independent of L_1 and L_3 such that*

$$\|v_1(\cdot,t)\|_\infty \le B_5[(L_1^2L_3^\rho + 1)|\chi| + 1],\ \forall\ t \in (0,T^*), \tag{2.31}$$

where $\rho \in (0,1)$ is as in Lemma 2.6.

Proof. We apply variation-of-constants formula to the first equation in (1.2) to calculate for all $t \in (0,T^*)$,

$$v_1(\cdot,t) \le e^{t(d_1\Delta - \mu)}v_{10} + |\chi|\int_0^t e^{(t-s)(d_1\Delta-\mu)}\nabla\cdot(v_1(\cdot,s)\nabla v_2(\cdot,s))ds + \Lambda^*\int_0^t e^{(t-s)(d_1\Delta-\mu)}ds.$$

Hence, by (iv) in Lemma 2.4 and the maximum principle,

$$\begin{aligned}\|v_1(\cdot,t)\|_\infty &\le \|v_{10}\|_\infty + |\chi|\int_0^t e^{-\mu(t-s)}\|e^{(t-s)d_1\Delta}\nabla\cdot(v_1(\cdot,s)\nabla v_2(\cdot,s))\|_\infty ds\\ &\quad +\Lambda^*\int_0^t e^{-\mu(t-s)}ds\\ &\le \|v_{10}\|_\infty + k_4|\chi|\int_0^t e^{-\mu(t-s)}(1+(t-s)^{-\frac{1}{2}-\frac{n}{2q}})\|\nabla\cdot(v_1(\cdot,s)\nabla v_2(\cdot,s))\|_q ds\\ &\quad +\Lambda^*\int_0^t e^{-\mu(t-s)}ds\\ &\le \|v_{10}\|_\infty + k_4 b_2|\chi|L_1(B_1+B_2L_1+B_3L_1L_3^\rho)+\tilde{N},\ \forall\ t\in(0,T^*). \end{aligned} \tag{2.32}$$

where $b_2 := \int_0^t e^{-d_1\mu(t-s)}(1+(t-s)^{-\frac{1}{2}-\frac{n}{2q}})ds$ due to $q>n$. As $L_3\ge 1$, by Cauchy's inequality, one gets

$$L_1 \le L_1^2+\frac{1}{4}\le L_1^2L_3^\rho+\frac{1}{4}.$$

As a consequence, (2.32) becomes

$$\|v_1(\cdot,t)\|_\infty \le \|v_{10}\|_\infty + \tilde{N} + k_4b_2\left[(B_1+B_2+B_3)L_1^2L_3^\rho+\frac{B_1}{4}\right]\chi.$$

Taking $B_5 := \max\left\{\|v_{10}\|_\infty+\tilde{N}, k_4b_2(B_1+B_2+B_3), \frac{k_4b_2B_1}{4}\right\}$, (2.31) follows. □

On the basis of the above conduction, we can get the global existence and boundedness of the solution by giving a constraint on the magnitude of χ.

Theorem 2.3. *Assume $v_{10}, v_{30}\in C(\bar{\Omega})$ and $v_{20}\in W^{1,q}(\Omega)$ for $q>n$. There exists a positive constant χ_0 such that whenever $|\chi|\le\chi_0$, model (1.2) admits a global classical nonnegative solution in the following sense:*

$$v_1, v_3\in C(\bar{\Omega}\times[0,\infty))\cap C^{2,1}(\bar{\Omega}\times(0,\infty)) \text{ and } v_2\in C([0,\infty);W^{1,q}(\Omega))\cap C^{2,1}(\bar{\Omega}\times(0,\infty)).$$

Moreover, there exists a positive constant L_0 depending on the initial data such that

$$\|v_1(\cdot,t)\|_\infty + \|v_2(\cdot,t)\|_{W^{1,q}(\Omega)} + \|v_3(\cdot,t)\|_\infty \le L_0,\ \forall\ t>0.$$

Proof. We choose $B_1>0$ large enough such that

$$L_1 > \|v_{10}\|_\infty,\ L_1\ge 4B_5. \tag{2.33}$$

On the other hand, we choose L_3 large enough such that

$$L_3 > \|v_{30}\|_\infty,\ L_3 \geq (8B_4L_1)^{\frac{1}{1-\rho}},\ L_3 \geq 4B_4. \tag{2.34}$$

Let

$$\chi_0 := \frac{L_1}{4B_5(L_1^2L_3^\rho + 1)}. \tag{2.35}$$

Given $|\chi| \leq \chi_0$, let (v_1, v_2, v_3) be the corresponding maximally extended solution of (1.2) in $\Omega \times (0, T_{\max})$ with $T_{\max} \leq \infty$. We then define

$$\Gamma := \{T \in (0, T_{\max}) : \|v_1(\cdot, t)\|_\infty \leq L_1,\ \|v_3(\cdot, t)\|_\infty \leq L_3,\ \forall\ t \in (0, T)\}.$$

The continuity of v_1 and v_3 guarantees that Γ is nonempty and $T^* = \sup \Gamma$ is a well-defined element of $(0, \infty]$. According to (2.33), (2.35), and Lemma 2.8, we can obtain

$$\|v_1(\cdot, t)\|_\infty \leq B_5(L_1^2L_3^\rho + 1)|\chi| + B_5 \leq \frac{L_1}{2},\ \forall\ t \in (0, T^*).$$

In view of (2.34) and Lemma 2.7, one has

$$\|v_3(\cdot, t)\|_\infty \leq B_4 + 2B_4L_1L_3^\rho \leq \frac{L_3}{2},\ \forall\ t \in (0, T^*).$$

It follows from the continuity of v_1 and v_3 again that $T = T_{\max}$ and

$$\|v_1(\cdot, t)\|_\infty \leq L_1,\ \|v_3(\cdot, t)\|_\infty \leq L_3,\ \forall\ t \in (0, T_{\max}).$$

Moreover,

$$\|\nabla v_2(\cdot, t)\|_q \leq B_1 + B_2L_1 + B_3L_1L_3^\rho,\ \forall\ t \in (0, T_{\max}).$$

An application of the Poincaré's inequality gives that

$$\|v_2\|_{W^{1,q}(\Omega)} \leq C(B_1 + B_2L_1 + B_3L_1L_3^\rho) =: L_2.$$

By Lemma 2.5, we infer that $T_{\max} = \infty$. We complete the proof by taking

$$L_0 := \max\{L_1, L_2, L_3\}.$$

□

2.3 The case of arbitrary χ

In this subsection, we consider the boundedness of the solution for arbitrary χ for $\Omega \subset \mathbb{R}^1$. In this case, $|\chi|$ can be large. First, we introduce the Gagliardo-Nirenberg interpolation inequality [31, 32].

Lemma 2.9. *(Gagliardo-Nirenberg interpolation inequality). Let r and s be integers fulfilling $0 \leq r < s$, and let $1 \leq p, q \leq \infty$, $0 < m \leq \infty$ and $\frac{r}{s} \leq c \leq 1$ such that*

$$\frac{1}{m} - \frac{r}{n} = c\left(\frac{1}{p} - \frac{s}{n}\right) + (1-c)\frac{1}{q}.$$

Then for any $u \in W^{s,p}(\Omega) \cap L^q(\Omega)$, there exists a positive constant C depending only on Ω, s, p, q, n satisfying the inequality

$$\|D^r u\|_m \leq C(\|D^s u\|_p^c \|u\|_q^{1-c} + \|u\|_q),$$

with the following exception: if $1 < p < \infty$ and $s - r - \frac{n}{p}$ is a nonnegative integer, then the above inequality holds only for c fulfilling $\frac{r}{s} \leq c < 1$.

By Lemma 2.9, similar to the proof of Lemma 3.6 (i) in [23], we immediately obtain the following estimates.

Lemma 2.10. *Let $\Omega \subset \mathbb{R}^1$ be a finite interval. For $q > 1$, $\epsilon > 0$, there holds*

$$\begin{cases} \|v_1 + 1\|_q^{\frac{2q}{q-1}} \leq C\|\nabla(v_1+1)^{\frac{1}{2}}\|_2^2 + C, \\ \|(v_1+1)\ln(v_1+1)\|_1 \leq \epsilon\|\nabla(v_1+1)^{\frac{1}{2}}\|_2^2 + C_\epsilon, \\ \|v_1+1\|_q^p \leq \epsilon\|\nabla(v_1+1)^{\frac{1}{2}}\|_2^2 + C_\epsilon, \ \forall p < \dfrac{2q}{q-1}. \end{cases} \tag{2.36}$$

Moreover, for all $q > 1$, there holds

$$\|v_2\|_q^{\frac{5q}{q-1}} \leq C(\|\Delta v_2\|_2^2 + \|\nabla v_2\|_2^2 + 1), \tag{2.37}$$

$$\|v_3\|_q^{\frac{5q}{q-1}} \leq C(\|\Delta v_3\|_2^2 + \|\nabla v_3\|_2^2 + 1). \tag{2.38}$$

Note that Lemma 2.5 is valid for all $\chi \neq 0$ guaranteeing the existence of the local solution for model (1.2). Based on Lemma 2.10, we explore the higher-order regularity of the solution.

Lemma 2.11. *Let $\Omega \subset \mathbb{R}^1$ be a finite interval. The local-in-time solution of (1.2) satisfies*

$$\|(v_1(\cdot,t)+1)\ln(v_1(\cdot,t)+1)\|_1 + \|\nabla v_2(\cdot,t)\|_2 + \|\nabla v_3(\cdot,t)\|_2 \le C,\ \forall\ t \in (0,T_{\max}). \quad (2.39)$$

Moreover, there exists a positive constant C such that

$$\|v_3(\cdot,t)\|_\infty \le C,\ \forall\ t \in (0,T_{\max}). \quad (2.40)$$

Proof. We test the first equation of (1.2) by $\ln(v_1+1)+1$ and then integrate by parts to derive that

$$\begin{aligned} &\frac{d}{dt}\int_\Omega (v_1+1)\ln(v_1+1)dx + 4d_1\int_\Omega |\nabla (v_1+1)^{\frac{1}{2}}|^2 dx \\ &+ \int_\Omega \left[\frac{\delta v_1 v_2}{1+\sigma v_2} + k v_1 \ln\left(1+\frac{\beta v_3}{k}\right)\right][\ln(v_1+1)+1]dx \\ =\ & \chi\int_\Omega [v_1 - \ln(v_1+1)]\Delta v_2 dx + \int_\Omega \Lambda[\ln(v_1+1)+1]dx,\ \forall\ t\in(0,T_{\max}). \end{aligned} \quad (2.41)$$

We test the second equation of (1.2) by Δv_2 and then integrate by parts to obtain

$$\begin{aligned} &\frac{1}{2}\frac{d}{dt}\int_\Omega |\nabla v_2|^2 dx + \theta\int_\Omega |\nabla v_2|^2 dx + d_2\int_\Omega |\Delta v_2|^2 dx \\ =\ & -\int_\Omega \left[\frac{\delta v_1 v_2}{1+\sigma v_2} + k v_1 \ln\left(1+\frac{\beta v_3}{k}\right)\right]\Delta v_2 dx,\ \forall\ t\in(0,T_{\max}). \end{aligned} \quad (2.42)$$

Similarly, testing the third equation of (1.2) by Δv_3 and then integrating by parts produce

$$\frac{1}{2}\frac{d}{dt}\int_\Omega |\nabla v_3|^2 dx + \alpha\int_\Omega |\nabla v_3|^2 dx + d_3\int_\Omega |\Delta v_3|^2 dx = -\gamma\int_\Omega v_2\Delta v_3 dx,\ \forall\ t\in(0,T_{\max}). \quad (2.43)$$

We now try to bound the terms on the right-hand sides of the equalities (2.41)-(2.43) in terms of the dissipation terms on their left-hand sides.

According to Cauchy's inequality and (2.36), one has

$$\begin{aligned} &\chi\int_\Omega [v_1 - \ln(v_1+1)]\Delta v_2 dx + \int_\Omega \Lambda[\ln(v_1+1)+1]dx \\ \le\ & \epsilon_1\int_\Omega [v_1-\ln(v_1+1)]^2 dx + \frac{\chi^2}{4\epsilon_1}\int_\Omega |\Delta v_2|^2 dx + \Lambda^*\epsilon_2\int_\Omega |\nabla(v_1+1)^{\frac{1}{2}}|^2 dx + \Lambda^* C_{\epsilon_2} \\ \le\ & \epsilon_1\int_\Omega (v_1+1)^2 dx + \frac{\chi^2}{4\epsilon_1}\int_\Omega |\Delta v_2|^2 dx + \Lambda^*\epsilon_2\int_\Omega |\nabla(v_1+1)^{\frac{1}{2}}|^2 dx + \Lambda^* C_{\epsilon_2} \\ \le\ & (C\epsilon_1 + \Lambda^*\epsilon_2)\int_\Omega |\nabla(v_1+1)^{\frac{1}{2}}|^2 dx + \frac{\chi^2}{4\epsilon_1}\int_\Omega |\Delta v_2|^2 dx + C\epsilon_1 + \Lambda^* C_{\epsilon_2}. \end{aligned} \quad (2.44)$$

Again applying Cauchy's inequality to the right-hand side terms in (2.42) leads to

$$\begin{aligned} & -\int_\Omega \left[\frac{\delta v_1 v_2}{1+\sigma v_2} + k v_1 \ln\left(1+\frac{\beta v_3}{k}\right)\right]\Delta v_2 dx \\ \leq\ & \frac{d_2}{2}\int_\Omega |\Delta v_2|^2 dx + \frac{(\delta^*)^2}{d_2}\int_\Omega v_1^2 v_2^2 dx + \frac{(\beta^*)^2}{d_2}\int_\Omega v_1^2 v_3^2 dx. \end{aligned} \tag{2.45}$$

For $q>6$, by Hölder's inequality and Young's inequality, one has

$$\begin{aligned} \int_\Omega v_1^2 v_2^2 dx &\leq \|v_1+1\|^2_{\frac{2q}{q-2}}\|v_2\|_q^2 \\ &\leq \epsilon_3\|v_2\|_q^{\frac{5q}{q-1}} + C_{\epsilon_3}\|v_1+1\|^{\frac{10q}{5q-2(q-1)}}_{\frac{2q}{q-2}} \\ &\leq C\epsilon_3\|\Delta v_2\|_2^2 + C\epsilon_3\|\nabla v_2\|_2^2 + C\epsilon_3 + \epsilon_4 C_{\epsilon_3}\|\nabla(v_1+1)^{\frac{1}{2}}\|_2^2 + C_{\epsilon_3,\epsilon_4}, \end{aligned} \tag{2.46}$$

where we use (2.36) and (2.37). Analogously, one has

$$\int_\Omega v_1^2 v_3^2 dx \leq C\epsilon_5\|\Delta v_3\|_2^2 + C\epsilon_5\|\nabla v_3\|_2^2 + C\epsilon_5 + \epsilon_6 C_{\epsilon_5}\|\nabla(v_1+1)^{\frac{1}{2}}\|_2^2 + C_{\epsilon_5,\epsilon_6}, \tag{2.47}$$

where (2.36) and (2.38) are used.

By Hölder's inequality and Young's inequality again, and according to (2.37), we have

$$\begin{aligned} -\gamma\int_\Omega v_2\Delta v_3 dx &\leq \frac{d_3}{2}\int_\Omega |\Delta v_3|^2 dx + \frac{\gamma^2}{2d_3}\int_\Omega v_2^2 dx \\ &\leq \frac{d_3}{2}\int_\Omega |\Delta v_3|^2 dx + \frac{\gamma^2}{2d_3}\|v_2\|_q^2 \\ &\leq \frac{d_3}{2}\int_\Omega |\Delta v_3|^2 dx + \frac{\gamma^2}{2d_3}\epsilon_7\|v_2\|_q^{\frac{5q}{q-1}} + C_{\epsilon_7}\frac{\gamma^2}{2d_3} \\ &\leq \frac{d_3}{2}\int_\Omega |\Delta v_3|^2 dx + \frac{\gamma^2}{2d_3}C\epsilon_7[\|\Delta v_2\|_2^2 + \|\nabla v_2\|_2^2 + 1] + C_{\epsilon_7}\frac{\gamma^2}{2d_3}. \end{aligned} \tag{2.48}$$

In summary, by (2.41), together with (2.44), one has for all $t\in(0,T_{\max})$,

$$\begin{aligned} & \frac{d}{dt}\int_\Omega (v_1+1)\ln(v_1+1)dx + 4d_1\int_\Omega |\nabla(v_1+1)^{\frac{1}{2}}|^2 dx \\ \leq\ & (C\epsilon_1+\Lambda^*\epsilon_2)\int_\Omega |\nabla(v_1+1)^{\frac{1}{2}}|^2 dx + \frac{\chi^2}{4\epsilon_1}\int_\Omega |\Delta v_2|^2 dx + C\epsilon_1 + \Lambda^* C_{\epsilon_2} \\ \leq\ & (C\epsilon_1+\Lambda^*\epsilon_2)\int_\Omega |\nabla(v_1+1)^{\frac{1}{2}}|^2 dx + C_1(\epsilon_1)\chi^2\int_\Omega |\Delta v_2|^2 dx + C_2(\epsilon_1,\epsilon_2). \end{aligned} \tag{2.49}$$

It follows from (2.42) and (2.45)-(2.47) that for all $t\in(0,T_{\max})$,

$$\begin{aligned} & \frac{1}{2}\frac{d}{dt}\int_\Omega |\nabla v_2|^2 dx + \theta\int_\Omega |\nabla v_2|^2 dx + d_2\int_\Omega |\Delta v_2|^2 dx \\ \leq\ & \frac{d_2}{2}\int_\Omega |\Delta v_2|^2 dx + \frac{(\delta^*)^2}{d_2}\left[C\epsilon_3\|\Delta v_2\|_2^2 + C\epsilon_3\|\nabla v_2\|_2^2 + C\epsilon_3 + \epsilon_4 C_{\epsilon_3}\|\nabla(v_1+1)^{\frac{1}{2}}\|_2^2 + C_{\epsilon_3,\epsilon_4}\right] \\ & + \frac{(\beta^*)^2}{d_2}\left[C\epsilon_5\|\Delta v_3\|_2^2 + C\epsilon_5\|\nabla v_3\|_2^2 + C\epsilon_5 + \epsilon_6 C_{\epsilon_5}\|\nabla(v_1+1)^{\frac{1}{2}}\|_2^2 + C_{\epsilon_5,\epsilon_6}\right]. \end{aligned} \tag{2.50}$$

According to (2.43) and (2.48), clearly, we have

$$\begin{aligned}
&\frac{1}{2}\frac{d}{dt}\int_\Omega |\nabla v_3|^2dx+\alpha\int_\Omega |\nabla v_3|^2dx+d_3\int_\Omega |\Delta v_3|^2dx\\
\leq\ & \frac{d_3}{2}\int_\Omega |\Delta v_3|^2dx+\frac{\gamma^2}{2d_3}C\epsilon_7\left[\|\Delta v_2\|_2^2+\|\nabla v_2\|_2^2+1\right]+C_{\epsilon_7}\frac{\gamma^2}{2d_3},\ \forall\ t\in(0,T_{\max}).
\end{aligned}\tag{2.51}$$

Taking $\epsilon_3=\frac{d_2\min\{2\theta,d_2\}}{8(\delta^*)^2C}$, $\epsilon_7=\frac{d_3\min\{2\theta,d_2\}}{4\gamma^2C}$, and $\epsilon_5=\frac{d_2\min\{2\alpha,d_3\}}{4(\beta^*)^2C}$, adding (2.50) and (2.51), we have

$$\begin{aligned}
&\frac{d}{dt}\int_\Omega(|\nabla v_2|^2+v_3|^2)dx\\
&+\frac{\min\{2\theta,d_2\}}{2}\int_\Omega(|\nabla v_2|^2+|\Delta v_2|^2)dx+\frac{\min\{2\alpha,d_3\}}{2}\int_\Omega(|\nabla v_3|^2+|\Delta v_3|^2)dx\\
\leq\ & 2\left(\frac{(\delta^*)^2C_{\epsilon_3}\epsilon_4}{d_2}+\frac{(\beta^*)^2C_{\epsilon_5}\epsilon_6}{d_2}\right)\int_\Omega|\nabla(v_1+1)^{\frac{1}{2}}|^2dx+C_3,\ \forall\ t\in(0,T_{\max}),
\end{aligned}\tag{2.52}$$

where C_3 is a positive constant depending on ϵ_3, ϵ_4, ϵ_5, and ϵ_6. Selecting $\epsilon_1=\frac{d_1}{C}$, $\epsilon_2=\frac{d_1}{\Lambda^*}$, $\epsilon_4=\frac{d_1d_2\min\{2\theta,d_2\}}{16(\delta^*)^2C_{\epsilon_3}C_1\chi^2}$ and $\epsilon_6=\frac{d_1d_2\min\{2\theta,d_2\}}{16(\beta^*)^2C_{\epsilon_5}C_1\chi^2}$, then multiplying (2.49) by $\min\{2\theta,d_2\}$ and (2.52) by $2C_1\chi^2$, adding the results, we obtain for all $t\in(0,T_{\max})$,

$$\begin{aligned}
&\frac{d}{dt}\int_\Omega\left[\min\{2\theta,d_2\}(v_1+1)\ln(v_1+1)+4C_1\chi^2(|\nabla v_2|^2+|\nabla v_3|^2)\right]dx\\
&+\int_\Omega\left\{\min\{2\theta,d_2\}[d_1(v_1+1)\ln(v_1+1)+2C_1\chi^2|\nabla v_2|^2]+2C_1\chi^2\min\{2\alpha,d_3\}|\nabla v_3|^2\right\}dx\\
&+\int_\Omega C_1\chi^2[\{\min\{2\theta,d_2\}|\Delta v_2|^2+2\min\{2\alpha,d_3\}|\Delta v_3|^2]dx\leq\min\{2\theta,d_2\}C_2+4C_1C_3\chi^2.
\end{aligned}$$

Solving this standard Gronwall's inequality, we directly obtain the uniform estimate (2.39). By Poincaré's inequality, we have

$$\|v_3(\cdot,t)\|_2\leq C\|\nabla v_3(\cdot,t)\|_2,\ \forall\ t\in(0,T_{\max}).$$

Hence, v_3 is bounded in $W^{1,2}(\Omega)$. Then the continuous embedding $W^{1,2}(\Omega)\subset L^\infty(\Omega)$ for $n=1$ says that

$$\|v_3(\cdot,t)\|_\infty\leq\|v_3(\cdot,t)\|_{W^{1,2}(\Omega)}\leq C,\ \forall\ t\in(0,T_{\max}).$$

□

Lemma 2.11 plays a crucial role in establishing the boundedness of the solution for $n=1$ and arbitrary χ. It should be noted that the subtle inequalities (2.46) and (2.47) only hold for $n=1$. If $n\neq1$, we cannot get the estimates as (2.46) and (2.47). Now, we dedicate to obtaining the boundedness of v_1 in $L^2(\Omega)$. The boundedness of ∇v_2 in $L^4(\Omega)$ is also derived.

Lemma 2.12. *For $\Omega \subset \mathbb{R}^1$, the local-in-time solution of (1.2) satisfies*

$$\|v_1(\cdot,t)\|_2 + \|\nabla v_2(\cdot,t)\|_4 \le C,\ \forall\ t \in (0, T_{\max}). \tag{2.53}$$

Proof. Multiplying the first equation of (1.2) by v_1 and integrating by parts leads to

$$\begin{aligned} & \frac{1}{2}\frac{d}{dt}\int_\Omega v_1^2 dx + d_1\int_\Omega |\nabla v_1|^2 dx + \int_\Omega \frac{\delta v_1^2 v_2}{1+\sigma v_2} dx + \int_\Omega k v_1^2 \ln\left(1+\frac{\beta v_3}{k}\right) dx \\ = & -\chi\int_\Omega v_1 \nabla v_1 \cdot \nabla v_2 dx + \int_\Omega \Lambda v_1 dx \\ \le & \frac{d_1}{4}\int_\Omega v_1^2 dx + \frac{\chi^2}{d_1}\int_\Omega v_1^2 |\nabla v_2|^2 dx + \Lambda^* \int_\Omega v_1 dx,\ \forall\ t \in (0, T_{\max}). \end{aligned}$$

We may invoke Lemma 2.1 to see that

$$\begin{aligned} & \frac{1}{2}\frac{d}{dt}\int_\Omega v_1^2 dx + \frac{3d_1}{4}\int_\Omega |\nabla v_1|^2 dx + \int_\Omega \frac{\delta v_1^2 v_2}{1+\sigma v_2} dx + \int_\Omega k v_1^2 \ln\left(1+\frac{\beta v_3}{k}\right) dx \\ \le & \frac{\chi^2}{d_1}\int_\Omega v_1^2 |\nabla v_2|^2 dx + \Lambda^* M_1,\ \forall\ t \in (0, T_{\max}). \end{aligned} \tag{2.54}$$

Taking gradient of the second equation of (1.2) and multiplying it by $\nabla v_1 |\nabla v_2|^2$ and then integrating by parts, we obtain

$$\begin{aligned} & \frac{1}{2}\frac{d}{dt}\int_\Omega |\nabla v_2|^4 dx + d_2\int_\Omega |\nabla|\nabla v_2|^2|^2 dx + 2d_2\int_\Omega |\nabla v_2|^2 |D^2 v_2|^2 dx + 2\theta\int_\Omega |\nabla v_2|^4 dx \\ = & d_2\int_{\partial\Omega} |\nabla v_2|^2 |\nabla v_2|^2 \cdot \mathbf{n} dS - 2\int_\Omega \frac{\delta v_1 v_2}{1+\sigma v_2}\Delta v_2 |\nabla v_2|^2 dx - 2\int_\Omega \frac{\delta v_1 v_2}{1+\sigma v_2}\nabla v_2 \cdot \nabla |\nabla v_2|^2 dx \\ & -2\int_\Omega k v_1 \ln\left(1+\frac{\beta v_3}{k}\right)\Delta v_2 |\nabla v_2|^2 dx - 2\int_\Omega k v_1 \ln\left(1+\frac{\beta v_3}{k}\right)\nabla v_2 \cdot \nabla |\nabla v_2|^2 dx \\ =: & \mathcal{I}_0 + \mathcal{I}_1 + \mathcal{I}_2 + \mathcal{I}_3 + \mathcal{I}_4,\ \forall\ t \in (0, T_{\max}), \end{aligned}$$

where we utilize the identity

$$2\nabla u \cdot \nabla \Delta u = \Delta |\nabla u|^2 - 2|D^2 u|^2.$$

Here, $|D^2 u|^2 = \sum_{i,j=1}^n |\frac{\partial^2 u}{\partial x_i \partial x_j}|^2$. With reference to [33], we can deal with the boundary term as follows

$$\begin{aligned} \mathcal{I}_0 & \le \epsilon\int_\Omega |\nabla|\nabla v_2|^2|^2 dx + C_\epsilon\left(\int_\Omega |\nabla v_2|^2 dx\right)^2 \\ & \le \epsilon_8\int_\Omega |\nabla|\nabla v_2|^2|^2 dx + C_{\epsilon_8}. \end{aligned}$$

Note that

$$\begin{aligned}\mathcal{I}_1+\mathcal{I}_2 &\leq 2\int_\Omega \frac{\delta^*}{\sigma}|v_1\Delta v_2||\nabla v_2|^2dx+2\int_\Omega \frac{\delta^*}{\sigma}|v_1\nabla v_2\cdot\nabla|\nabla v_2|^2|dx\\ &\leq \frac{d_2}{n}\int_\Omega |\Delta v_2|^2|\nabla v_2|^2dx+\frac{n(\frac{\delta^*}{\sigma})^2}{d_2}\int_\Omega v_1^2|\nabla v_2|^2dx\\ &\quad+\frac{d_2}{4}\int_\Omega |\nabla|\nabla v_2|^2|^2dx+\frac{4(\frac{\delta^*}{\sigma})^2}{d_2}\int_\Omega v_1^2|\nabla v_2|^2dx.\end{aligned}$$

Similarly, one has

$$\begin{aligned}\mathcal{I}_3+\mathcal{I}_4 &\leq 2\int_\Omega |\beta^* v_1v_3\Delta v_2||\nabla v_2|^2dx+2\int_\Omega |\beta^* v_1v_3\nabla v_2\cdot\nabla|\nabla v_2|^2|dx\\ &\leq \frac{d_2}{n}\int_\Omega |\Delta v_2|^2|\nabla v_2|^2dx+\frac{n(\beta^*)^2\|v_3\|_\infty^2}{d_2}\int_\Omega v_1^2|\nabla v_2|^2dx\\ &\quad+\frac{d_2}{4}\int_\Omega |\nabla|\nabla v_2|^2|^2dx+\frac{4(\beta^*)^2\|v_3\|_\infty^2}{d_2}\int_\Omega v_1^2|\nabla v_2|^2dx.\end{aligned}$$

As a result, we conclude that

$$\begin{aligned}\sum_{i=0}^4\mathcal{I}_i &\leq 2d_2\int_\Omega |D^2v_2|^2|\nabla v_2|^2dx+\left(\frac{d_2}{2}+\epsilon_8\right)\int_\Omega |\nabla|\nabla v_2|^2|^2dx\\ &\quad+\frac{n+4}{d_2}\left(\left(\frac{\delta^*}{\sigma}\right)^2+(\beta^*)^2\|v_3\|_\infty^2\right)\int_\Omega v_1^2|\nabla v_2|^2dx+C_{\epsilon_8}. \qquad (2.55)\end{aligned}$$

Now, by one-dimensional Gagliardo-Nirenberg interpolation inequality, for $q>1$, $p<\frac{3q}{q-1}$, we know

$$\|v_1\|_q^p\leq\epsilon\|\nabla v_1\|_2^2+C_\epsilon,$$

and

$$\||\nabla v_2|^2\|_q^{\frac{3q}{q-1}}\leq C\|\nabla|\nabla v_2|^2\|_2^2+C.$$

Thus, combining with the above inequalities, we get

$$\begin{aligned}\int_\Omega v_1^2|\nabla v_2|^2dx &\leq \|v_1\|_{\frac{2q}{q-1}}^2\||\nabla v_2|^2\|_q\\ &\leq \epsilon_9\||\nabla v_2|^2\|_q^{\frac{3q}{q-1}}+C_{\epsilon_9}\|v_1\|_{\frac{2q}{q-1}}^{\frac{6q}{2q+1}}\\ &\leq C_4\epsilon_9\||\nabla v_2|^2\|_2^2+C_4\epsilon_9+\epsilon_{10}C_{\epsilon_9}\|\nabla v_1\|_2^2+C_{\epsilon_9,\epsilon_{10}}. \qquad (2.56)\end{aligned}$$

Therefore, in view of (2.55), it is clear for all $t \in (0, T_{\max})$ that

$$\frac{1}{2}\frac{d}{dt}\int_\Omega |\nabla v_2|^4 dx + \frac{d_2}{4}\int_\Omega |\nabla|\nabla v_2|^2|^2 dx + 2\theta\int_\Omega |\nabla v_2|^4 dx \le \epsilon_{11}\int_\Omega |\nabla v_1|^2 dx + C_{\epsilon_{11}}. \quad (2.57)$$

Moreover, taking $\epsilon_{10} = \frac{d_1^2}{4C_{\epsilon_9}\chi^2}$ and substituting (2.56) to (2.54) yield

$$\begin{aligned} &\frac{1}{2}\frac{d}{dt}\int_\Omega v_1^2 dx + \frac{d_1}{2}\int_\Omega |\nabla v_1|^2 dx + \int_\Omega \frac{\delta v_1^2 v_2}{1+\sigma v_2} dx + \int_\Omega k v_1^2 \ln\left(1+\frac{\beta v_3}{k}\right) dx \\ \le\ & C_5\int_\Omega |\nabla|\nabla v_2|^2|^2 dx + C_6,\ \forall\ t \in (0, T_{\max}), \end{aligned} \quad (2.58)$$

where C_5 depending on ϵ_9 and C_6 depending on ϵ_9 and ϵ_{10} are positive constants.

We multiply (2.57) by $\frac{8C_5}{d_2}$ to annihilate the first term on the right-hand side of (2.58). The choice of ϵ_{11} is done in such a way that $\frac{d_1}{2} - \frac{8C_5\epsilon_{11}}{d_2} = \frac{d_1}{4}$. We then observe that

$$\begin{aligned} &\frac{d}{dt}\int_\Omega (v_1^2 + |\nabla v_2|^4) dx \\ &+C\int_\Omega \left(|\nabla v_1|^2 + |\nabla v_2|^2 + |\nabla|\nabla v_2|^2| + \frac{\delta v_1^2 v_2}{1+\sigma v_2} + k v_1^2 \ln\left(1+\frac{\beta v_3}{k}\right)\right) dx \\ \le\ & C,\ \forall\ t \in (0, T_{\max}). \end{aligned}$$

We employ Poincaré inequality in estimating

$$\begin{aligned} &\frac{d}{dt}\int_\Omega (v_1^2 + |\nabla v_2|^4) dx + C\int_\Omega \left(\frac{\delta v_1^2 v_2}{1+\sigma v_2} + k v_1^2 \ln\left(1+\frac{\beta v_3}{k}\right)\right) dx \\ \le\ & -C\int_\Omega (v_1^2 + |\nabla v_2|^4) dx + C,\ \forall\ t \in (0, T_{\max}). \end{aligned}$$

Then by Gronwall's inequality, (2.53) is readily derived. □

Since the spatial dimension is one, we can get the boundedness of the solution without any restriction on χ.

Theorem 2.4. *For $\Omega \subset \mathbb{R}^1$, assume $v_{10}, v_{30} \in C(\bar{\Omega})$ and $v_{20} \in W^{1,q}(\Omega)$ for $q > 1$. Then there exists a unique global classical solution of (1.2) in the sense of Theorem 2.3.*

Proof. We employ the boundedness of v_1 in $L^2(\Omega)$ and v_3 in $L^\infty(\Omega)$ to derive the boundedness of ∇v_2 and v_1 in $L^\infty(\Omega)$. Applying the variation-of-constants formula and then taking the

gradient for the second equation, one has

$$\begin{aligned}
\|\nabla v_2(\cdot,t)\|_\infty &\le \|\nabla e^{t(d_2\Delta-\theta)}v_{20}\|_\infty + \int_0^t \left\|\nabla e^{(t-s)(d_2\Delta-\theta)}\left[\frac{\delta v_1 v_2}{1+\sigma v_2} + kv_1\ln\left(1+\frac{\beta v_3}{k}\right)\right]\right\|_\infty ds \\
&\le C\|\nabla v_{20}\|_\infty + \int_0^t \left\|\nabla e^{(t-s)(d_2\Delta-\theta)}\left(\frac{\delta^*}{\sigma}+\beta^* v_3\right)v_1\right\|_\infty ds \\
&\le C\|\nabla v_{20}\|_\infty + \int_0^t k_2[1+(t-s)^{-\frac{1}{2}-\frac{1}{4}}]e^{-\theta(t-s)}\left(\frac{\delta^*}{\sigma}+\beta^*\|v_3\|_\infty\right)\|v_1\|_2 ds \\
&\le C + C\int_0^\infty (1+\tau^{-\frac{3}{4}})e^{-\theta\tau}d\tau \\
&\le C,\ \forall\ t\in(0,T_{\max}), \qquad (2.59)
\end{aligned}$$

where we have used Lemma 2.4 (ii) and the estimate (2.40). Applying the variation-of-constants formula to the first equation of (1.2), we have

$$\begin{aligned}
v_1(\cdot,t) &= e^{t(d_1\Delta-\mu)}v_{10} + \chi\int_0^t e^{(t-s)(d_1\Delta-\mu)}\nabla\cdot(v_1\nabla v_2)ds \\
&\quad + \int_0^t e^{(t-s)(d_1\Delta-\mu)}\left[\Lambda - \frac{\delta v_1 v_2}{1+\sigma v_2} - kv_1\ln\left(1+\frac{\beta v_3}{k}\right)\right]ds,\ \forall\ t\in(0,T_{\max}).
\end{aligned}$$

By use of Lemmas 2.4, 2.11 and 2.12, we proceed to check that

$$\begin{aligned}
\|v_1(\cdot,t)\|_\infty &\le \|e^{t(d_1\Delta-\mu)}v_{10}\|_\infty + |\chi|\int_0^t \|e^{(t-s)(d_1\Delta-\mu)}\nabla\cdot(v_1\nabla v_2)\|_\infty ds \\
&\quad + \int_0^t \left\|e^{(t-s)(d_1\Delta-\mu)}\left[\Lambda + \frac{\delta v_1 v_2}{1+\sigma v_2} + kv_1\ln\left(1+\frac{\beta v_3}{k}\right)\right]\right\|_\infty ds \\
&\le C + k_4|\chi|\int_0^t (1+(t-s)^{-\frac{1}{2}-\frac{1}{4}})e^{-\mu(t-s)}\|v_1\nabla v_2\|_2 ds \\
&\quad + k_1\int_0^t (1+(t-s)^{-\frac{1}{4}})e^{-\mu(t-s)}\left[\Lambda^* + \left(\frac{\delta^*}{\sigma}+\beta^*\|v_3\|_\infty\right)\|v_1\|_2\right]ds \\
&\le C,\ \forall\ t\in(0,T_{\max}). \qquad (2.60)
\end{aligned}$$

By (2.40) and (2.60), we know that v_1 and v_3 are bounded in $L^\infty(\Omega)$. By (2.59), v_2 is bounded in $W^{1,q}(\Omega)$ for $t\in[0,T_{\max})$ and $q>1$. Then by Lemma 2.5, we conclude $T_{\max}=\infty$, implying the global existence and boundedness of the solution. □

We make a brief summary of the existence and boundedness of the solution to model (1.2). When there is no chemotaxis, we establish the global existence of the solution. Furthermore, the ultimate boundedness and the existence of a global attractor are also derived. When $|\chi|$ is sufficiently small, the global existence of the solution is obtained for all n. As a compromise,

when there is no restriction on χ, we can only acquire the global existence of the solution for $n = 1$.

3 Threshold dynamics

We now demonstrate the threshold dynamics of model (1.2) in terms of the basic reproduction number.

3.1 Basic reproduction number

It follows from Lemma 1 in [27] that (1.2) admits a pathogen-free equilibrium $E_0 = (V, 0, 0)$, where V is the unique positive solution of

$$\begin{cases} d_1 \Delta v_1 + \Lambda(x) - \mu v_1 = 0, & x \in \Omega, \\ \nabla v_1 \cdot \mathbf{n} = 0, & x \in \partial\Omega. \end{cases}$$

We linearize (1.2) at E_0 to get

$$\begin{cases} \partial_t v_1 - d_1 \Delta v_1 = -\mu v_1 - \delta(x) V v_2 - \beta(x) V v_3, & x \in \Omega,\ t > 0, \\ \partial_t v_2 - d_2 \Delta v_2 = \delta(x) V v_2 + \beta(x) V v_3 - \theta v_2, & x \in \Omega,\ t > 0, \\ \partial_t v_3 - d_3 \Delta v_3 = \gamma v_2 - \alpha v_3, & x \in \Omega,\ t > 0, \\ \nabla v_1 \cdot \mathbf{n} = \nabla v_2 \cdot \mathbf{n} = \nabla v_3 \cdot \mathbf{n} = 0, & x \in \partial\Omega,\ t > 0, \\ v_1(x, 0) = v_{10}(x),\ v_2(x, 0) = v_{20}(x),\ v_3(x, 0) = v_{30}(x), & x \in \Omega. \end{cases} \tag{3.1}$$

Following the next-generation-operator approach [34], by virtue of (3.1), we define $L = \mathrm{diag}(-d_2\Delta, -d_3\Delta)$,

$$F(x) = \begin{pmatrix} \delta V & \beta V \\ 0 & 0 \end{pmatrix},\ V(x) = \begin{pmatrix} \theta & 0 \\ -\gamma & \alpha \end{pmatrix}.$$

Let $\Psi(t) : C(\bar{\Omega}, \mathbb{R}^2) \to C(\bar{\Omega}, \mathbb{R}^2)$ be the solution semigroup generated by $L - V$. Suppose that the distribution of initial infection is $\psi(x) = (\psi_2(x), \psi_3(x))$. Then the distribution of new infectives is

$$\mathcal{L}(\psi)(x) := \int_0^\infty F(x)\Psi(t)\psi dt.$$

Hence, the basic reproduction number of (1.2) is defined by

$$\mathcal{R}_0 := r(\mathcal{L}),$$

where $r(\mathcal{L})$ is the spectral radius of $\mathcal{L}$. It then follows from standard arguments in the theory of dynamical system [8, 35] that we have the following threshold dynamics in terms of $\mathcal{R}_0$.

Proposition 3.1. *The following assertions hold.*

(i) For arbitrary χ, if $\mathcal{R}_0 < 1$, then E_0 is globally asymptotically stable.

(ii) For zero χ, if $\mathcal{R}_0 > 1$, then system (1.2) is uniformly persistent. Moreover, (1.2) admits at least one positive steady state.

With reference to Theorem 3.4 in [34], we can define the basic reproduction number for model (1.2) in a spatially homogeneous environment.

Proposition 3.2. *If $\Lambda(x)$, $\delta(x)$, and $\beta(x)$ are independent of the position x, then*

$$\mathcal{R}_0 = \frac{\delta\Lambda}{\mu\theta} + \frac{\beta\Lambda\gamma}{\mu\alpha\theta}. \tag{3.2}$$

The first part of $\mathcal{R}_0$ denotes the infection spread by infected hosts, as $\mathcal{R}_0$ gets larger with δ increasing. The second part of $\mathcal{R}_0$ represents the disease transmission from pathogens. $\mathcal{R}_0$ fluctuates in response to the changes of β.

3.2 A limiting case

In this subsection, we explore the limiting case when $\sigma \to 0$ and $k \to \infty$ in (1.2) with Λ, δ, and β independent of x. Model (1.2) is then written as

$$\begin{cases} \partial_t v_1 - d_1\Delta v_1 = \chi\nabla\cdot(v_1\nabla v_2) + \Lambda - \mu v_1 - \delta v_1 v_2 - \beta v_1 v_3, & x \in \Omega,\ t > 0, \\ \partial_t v_2 - d_2\Delta v_2 = \delta v_1 v_2 + \beta v_1 v_3 - \theta v_2, & x \in \Omega,\ t > 0, \\ \partial_t v_3 - d_3\Delta v_3 = \gamma v_2 - \alpha v_3, & x \in \Omega,\ t > 0, \\ \nabla v_1 \cdot \mathbf{n} = \nabla v_2 \cdot \mathbf{n} = \nabla v_3 \cdot \mathbf{n} = 0, & x \in \partial\Omega,\ t > 0, \\ v_1(x,0) = v_{10}(x),\ v_2(x,0) = v_{20}(x),\ v_3(x,0) = v_{30}(x), & x \in \Omega. \end{cases} \tag{3.3}$$

The basic reproduction number for (3.3) can be defined as identical to (3.2). The pathogen-free equilibrium of (3.3) is $E_1 = (\frac{\Lambda}{\mu}, 0, 0)$. If $\mathcal{R}_0 > 1$, the endemic equilibrium of (3.3) is $E^* = (v_1^*, v_2^*, v_3^*)$, where

$$v_1^* = \frac{\alpha\theta}{\delta\alpha + \beta\gamma},\ v_2^* = \frac{\Lambda - \mu v_1^*}{\theta},\ v_3^* = \frac{\gamma v_2^*}{\alpha}.$$

We now consider the case $\chi < 0$, which represents the chemotactic attraction between the hosts. In order to analyze the Turing pattern formation of (3.3), we then work with a non-dimensional version of (3.3) to reduce the number of parameters and simplify some of the analysis. The non-dimensional dependent species variables are given by

$$V_1 = \frac{v_1}{v_1^*},\ V_2 = \frac{v_2}{v_2^*},\ V_3 = \frac{v_3}{v_3^*},$$

and the non-dimensional space variable $X = (X_1, ..., X_n) \in \mathbb{R}^n$ and time variable $\tau \in \mathbb{R}$ are set as

$$\tau = \frac{t}{H_t},\ X_i = \frac{x_i}{H},\ i = 1, ..., n,$$

where H and H_t are positive constants which will be chosen later. Substitute the non-dimensional variables into (3.3) to get

$$\begin{cases} \partial_\tau V_1 - \dfrac{d_1 H_t}{H^2}\Delta V_1 = \dfrac{\chi H_t v_2^*}{H^2}\nabla\cdot(V_1\nabla V_2) + \dfrac{H_t\Lambda}{v_1^*} - \mu H_t V_1 & \\ \qquad\qquad - \delta H_t v_2^* V_1 V_2 - \beta H_t v_3^* V_1 V_3, & X \in \tilde{\Omega},\ \tau > 0, \\ \partial_\tau V_2 - \dfrac{d_2 H_t}{H^2}\Delta V_2 = \delta H_t v_1^* V_1 V_2 + \dfrac{\beta H_t v_1^* v_3^*}{v_2^*} V_1 V_3 - \theta H_t V_2, & X \in \tilde{\Omega},\ \tau > 0, \\ \partial_\tau V_3 - \dfrac{d_3 H_t}{H^2}\Delta V_3 = \dfrac{\gamma H_t v_2^*}{v_3^*} V_2 - \alpha H_t V_3, & X \in \tilde{\Omega},\ \tau > 0, \\ \nabla V_1 \cdot \mathbf{n} = \nabla V_2 \cdot \mathbf{n} = \nabla V_3 \cdot \mathbf{n} = 0, & X \in \partial\tilde{\Omega},\ t > 0, \\ V_1(X, 0) = V_{10}(X),\ V_2(X, 0) = V_{20}(X),\ V_3(X, 0) = V_{30}(X), & X \in \tilde{\Omega}, \end{cases} \tag{3.4}$$

where $\tilde{\Omega} = \left\{ \dfrac{x}{H} :\ x \in \Omega \right\}$. Let

$$H_t := \frac{1}{\mu},\ H^2 := \frac{d_1}{\mu},\ \tilde{\Lambda} = \frac{\Lambda}{\mu v_1^*},\ \tilde{\chi} := \frac{\chi H_t v_2^*}{H^2},\ \tilde{\theta} := \frac{\theta}{\mu},$$

$$D_2 := \frac{d_2 H_t}{H^2},\ D_3 := \frac{d_3 H_t}{H^2},\ \tilde{\delta} := \frac{\delta v_2^*}{\mu},\ \tilde{\beta} := \frac{\beta v_1^* v_3^*}{\mu v_2^*},\ \tilde{\alpha} = \frac{\alpha}{\mu}.$$

Then (3.4) becomes

$$\begin{cases} \partial_\tau V_1 - \Delta V_1 = \tilde{\chi}\nabla\cdot(V_1\nabla V_2) + \tilde{\Lambda} - V_1 - \tilde{\delta}V_1V_2 - (\tilde{\Lambda} - 1 - \tilde{\delta})V_1V_3, & X \in \tilde{\Omega},\ \tau > 0, \\ \partial_\tau V_2 - D_2\Delta V_2 = (\tilde{\theta} - \tilde{\beta})V_1V_2 + \tilde{\beta}V_1V_3 - \tilde{\theta}V_2, & X \in \tilde{\Omega},\ \tau > 0, \\ \partial_\tau V_3 - D_3\Delta V_3 = \tilde{\alpha}(V_2 - V_3), & X \in \tilde{\Omega},\ \tau > 0, \\ \nabla V_1\cdot\mathbf{n} = \nabla V_2\cdot\mathbf{n} = \nabla V_3\cdot\mathbf{n} = 0, & X \in \partial\tilde{\Omega},\ t > 0, \\ V_1(X,0) = V_{10}(X),\ V_2(X,0) = V_{20}(X),\ V_3(X,0) = V_{30}(X), & X \in \tilde{\Omega}. \end{cases} \tag{3.5}$$

After simplifying (3.3), it is straightforward to check that in the absence of spatial variation (3.5) admits the following two equilibria: pathogen-free equilibrium $E_1 = (\tilde{\Lambda}, 0, 0)$, and endemic equilibrium $E^* = (1, 1, 1)$ for $\tilde{\Lambda} > 1$.

The Jacobian matrix of (3.5) at E^* is

$$\mathcal{J}(E^*) = \begin{pmatrix} -\tilde{\Lambda} - l^2 & -\tilde{\delta} + \tilde{\chi}l^2 & -(\tilde{\Lambda} - 1 - \tilde{\delta}) \\ \tilde{\theta} & \tilde{\beta} - D_2l^2 & \tilde{\beta} \\ 0 & \tilde{\alpha} & -\tilde{\alpha} - D_3l^2 \end{pmatrix}.$$

Here, $l^2 := \mathbf{l}^{\mathrm{T}}\mathbf{l}$, where $\mathbf{l} \in \mathbb{R}^n$ is the wave number. The corresponding characteristic polynomial of $\mathcal{J}(E^*)$ is

$$\begin{aligned} P(\lambda) &= \lambda^3 + \lambda^2\left[(1 + D_2 + D_3)l^2 + (\tilde{\alpha} + \tilde{\beta} + \tilde{\Lambda})\right] \\ &\quad + \lambda\Big[(D_2 + D_3 + D_2D_3)l^4 + \left(D_2\tilde{\alpha} + D_3\tilde{\beta} + (D_2 + D_3)\tilde{\Lambda} + \tilde{\alpha} + \tilde{\beta} + \tilde{\chi}\tilde{\theta}\right)l^2 \\ &\quad + \left((\tilde{\alpha} + \tilde{\beta})\tilde{\Lambda} + \tilde{\delta}\tilde{\theta}\right)\Big] + \Big[D_2D_3l^6 + \left(D_2\tilde{\alpha} + D_3\tilde{\beta} + D_2D_3\tilde{\Lambda} + \tilde{\chi}\tilde{\theta}D_3\right)l^4 \\ &\quad + \left((D_2\tilde{\alpha} + D_3\tilde{\beta})\tilde{\Lambda} + D_2\tilde{\delta} + \tilde{\chi}\tilde{\alpha}\right)l^2 + \tilde{\alpha}\tilde{\theta}(\tilde{\Lambda} - 1)\Big] \\ &=: \lambda^3 + f\lambda^2 + g\lambda + h, \end{aligned}$$

where

$$f = (1 + D_2 + D_3)l^2 + (\tilde{\alpha} + \tilde{\beta} + \tilde{\Lambda}) =: f_1l^2 + f_2,$$

$$\begin{aligned} g &= (D_2 + D_3 + D_2D_3)l^4 + \left(D_2\tilde{\alpha} + D_3\tilde{\beta} + (D_2 + D_3)\tilde{\Lambda} + \tilde{\alpha} + \tilde{\beta} + \tilde{\chi}\tilde{\theta}\right)l^2 + \left((\tilde{\alpha} + \tilde{\beta})\tilde{\Lambda} + \tilde{\delta}\tilde{\theta}\right) \\ &=: g_1l^4 + g_2l^2 + g_3, \end{aligned}$$

$$
\begin{aligned}
h &= D_2D_3l^6 + \left(D_2\tilde{\alpha} + D_3\tilde{\beta} + D_2D_3\tilde{\Lambda} + \tilde{\chi}\tilde{\theta}D_3\right)l^4 + \left((D_2\tilde{\alpha} + D_3\tilde{\beta})\tilde{\Lambda} + D_2\tilde{\delta} + \tilde{\chi}\tilde{\alpha}\right)l^2 \\
&\quad + \tilde{\alpha}\tilde{\theta}(\tilde{\Lambda} - 1) \\
&=: h_1l^6 + h_2l^4 + h_3l^2 + h_4.
\end{aligned}
$$

It is obvious that f_1, f_2, g_1, g_3, h_1, and h_4 are positive, while g_2, h_2, and h_3 may be nonpositive. Note that patterns may occur in a reaction-chemotaxis-diffusion system in the neighborhood of a spatially homogeneous steady state provided the conditions for the chemotaxis-driven instability are satisfied. The conditions are:

(A1) The steady state is linearly stable in the absence of diffusion and chemotaxis;

(A2) The steady state is linearly unstable in the presence of diffusion and chemotaxis.

It follows from Theorem 4 in [36] that (A1) is satisfied for $l^2 = 0$. According to the Ruth-Hurwitz stability criterion for a cubic polynomial, we know E^* is stable if and only if $f, g, h > 0$ and $fg > h$. Thus we give the necessary conditions to guarantee (A2) holds for the steady state of (3.3) as follows.

Proposition 3.3. *Given $\chi < 0$, the chemotaxis-driven instability occurs for (3.3) if at least one of the following conditions holds:*

(i) $\chi \le -\left(\dfrac{(d_1+d_2)\alpha}{\theta v_2^*} + \dfrac{(d_1+d_3)\beta\gamma v_1^*}{\alpha\theta v_2^*} + \dfrac{(d_2+d_3)\Lambda}{\theta v_1^* v_2^*}\right)$;

(ii) $\chi \le -\left(\dfrac{d_1d_2\alpha}{d_3\theta v_2^*} + \dfrac{d_1\beta\gamma v_1^*}{\alpha\theta v_2^*} + \dfrac{d_2\Lambda}{\theta v_1^* v_2^*}\right)$;

(iii) $\chi \le -\left(\dfrac{d_2\Lambda}{\mu v_1^* v_2^*} + \dfrac{d_3\beta\gamma\Lambda}{\mu\alpha^2 v_2^*} + \dfrac{d_3\delta}{\alpha}\right)$.

Proof. Applying the Ruth-Hurwitz stability criterion for $P(\lambda)$, we can infer that one way that E^* of (3.5) may become unstable is at least one of g_2, h_2, and h_3 is nonpositive. Thus, either

(P1) $g_2 \le 0$, i.e., $\tilde{\chi} \le -\left(\dfrac{D_2\tilde{\alpha}}{\tilde{\theta}} + \dfrac{D_3\tilde{\beta}}{\tilde{\theta}} + \dfrac{\tilde{\alpha}+\tilde{\beta}}{\tilde{\theta}}\right)$; or

(P2) $h_2 \le 0$, i.e., $\tilde{\chi} \le -\left(\dfrac{D_2\tilde{\alpha}}{D_3\tilde{\theta}} + \dfrac{\tilde{\beta}}{\tilde{\theta}} + \dfrac{D_1\tilde{\Lambda}}{\tilde{\theta}}\right)$; or

(P3) $h_3 \le 0$, i.e., $\tilde{\chi} \le -\left(D_2\tilde{\Lambda} + \dfrac{D_3\tilde{\beta}\tilde{\Lambda}}{\tilde{\alpha}} + \dfrac{D_3\tilde{\delta}}{\tilde{\alpha}}\right)$.

As a consequence, conditions (i)-(iii) in Proposition 3.3 are equivalent to conditions (P1)-(P3). □

4 Spatial aggregation and segregation

We now proceed to verify the results of boundedness for different χ numerically within one- and two-dimensional domains. Additionally, spatial aggregation and segregation phenomena will be illustrated.

4.1 Spatial aggregation

In this subsection, the parameter values are taken as follows: $d_1 = d_2 = k = \sigma = \alpha = 1$, $d_3 = \mu = 0.1$, $\Lambda = 10$, $\gamma = 2$, and $\theta = 0.5$. For the one-dimensional simulation, we take Ω as a finite open interval $\Omega_1 := \Omega = (-10, 10)$. For the two-dimensional simulation, model (1.2) will be numerically solved on a square domain $\Omega_2 := \Omega = (-10, 10) \times (-10, 10)$.

We first consider the case without chemotaxis in model (1.2). For the one-dimensional simulation, the initial values are taken as $(v_{10}, v_{20}, v_{30}) = (100e^{-|x|^2}, 10e^{-|x|^2}, 50e^{-|x|^2})$, $x \in \Omega_1$, and we assume

$$\delta(x) = 0.3\cos x + 0.32,\ \beta(x) = 0.5\sin x + 0.53,\ x \in \Omega_1.$$

For the two-dimensional simulation, the initial values are taken as $(v_{10}, v_{20}, v_{30}) = (100, 10, 50)$, $(x, y) \in \Omega_2$, and we assume

$$\delta(x, y) = 0.0003\cos x \sin y + 0.16,\ \beta(x, y) = 0.0005\sin x \cos y + 0.1,\ (x, y) \in \Omega_2.$$

Actually, the parameter values chosen in this way guarantee that $\mathcal{R}_0 > 1$ by Proposition 3.2.

When the chemotaxis is absent in model (1.2), that is, $\chi = 0$, the numerical results are depicted in Fig. 1. By observing Fig. 1(a)-(c), at the initial stage, both the hosts and pathogens are highly concentrated in the neighborhood of $x = 0$. However, the solution tends to a steady state as time evolves. Fig. 1(d)-(f) illustrates the spatial distribution of infected hosts in a square at different time moments. Since the infection rates are taken as periodic functions of spatial variables x and y, the solution also performs periodicity at the steady state, as displayed in Fig. 1(g)-(i). The solution remains bounded regardless of the spatial dimension of the domain, and its ultimate bound is independent of the initial data, which are consistent with Theorems 2.1 and 2.2.

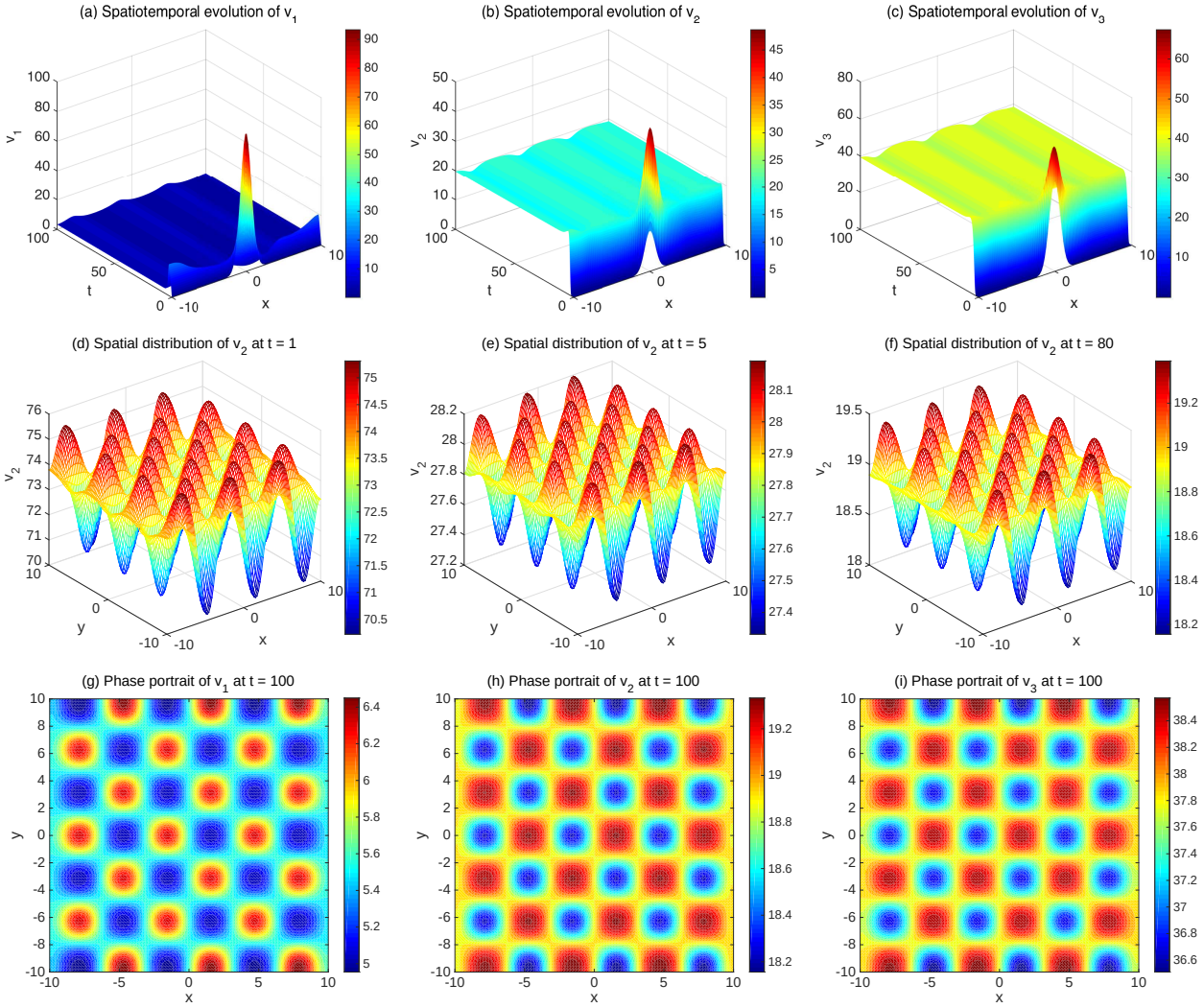

Fig. 1: $\chi = 0$ in model (1.2). (a)-(c): the spatiotemporal evolution of the solution for the one-dimensional domain. (d)-(f): the spatial distribution of v_2 at $t = 1, 5, 80$ for the two-dimensional domain, respectively. (g)-(i): the phase portraits of the solution at the steady state.

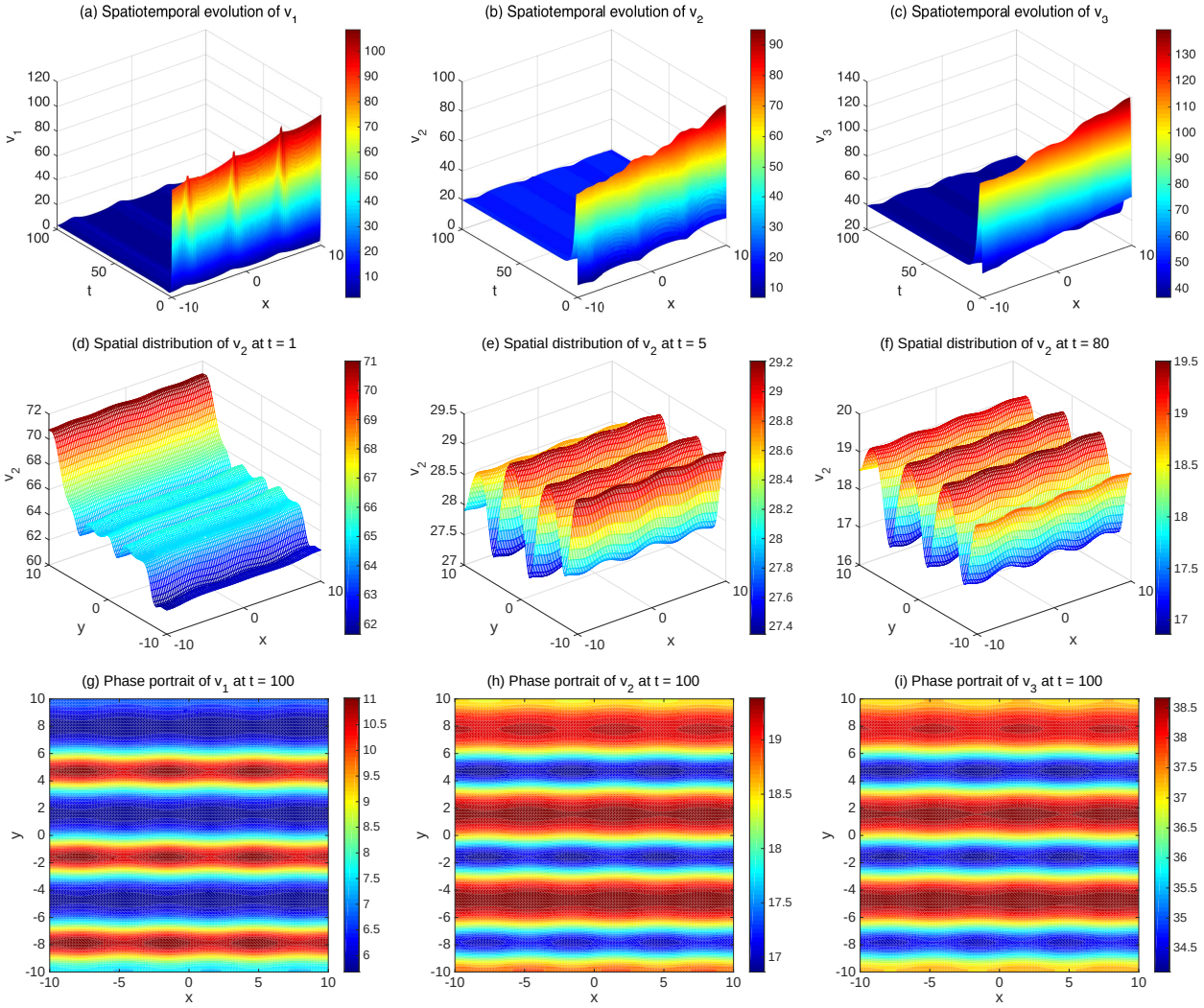

Fig. 2: $\chi = 0.1$ in model (1.2). (a)-(c): the spatiotemporal evolution of the solution for the one-dimensional domain. (d)-(f): the spatial distribution of v_2 at $t = 1, 5, 80$ for the two-dimensional domain, respectively. (g)-(i): the phase portraits of the solution at the steady state.

We then explore the case of weak chemotaxis by taking $\chi = 0.1$. For the one-dimensional simulation, the initial data are taken as $(v_{10}, v_{20}, v_{30}) = (100 + x, 10 + 0.5x, 50 + x),\ x \in \Omega_1$, and the infection rates are

$$\delta(x) = 0.3\cos x + 0.32,\ \beta(x) = 0.5\sin x + 0.53,\ x \in \Omega_1.$$

For the two-dimensional simulation, the initial data are the same as those in the case without chemotaxis, and the infection rates are taken in this way:

$$\delta(x) = 0.03\sin x + 0.05,\ \beta(y) = 0.05\sin y + 0.07,\ (x, y) \in \Omega_2,$$

where the infection rate of infected hosts is periodic in x, whereas the infection rate of pathogens is periodic in y.

The numerical results are presented in Fig. 2. From Fig. 2(a)-(c), the hosts and pathogens highly concentrate at the position $x = 10$, while the distribution of the steady state behaves periodically in x. Fig. 2(d)-(f) shows the spatial distribution of the infected hosts at different time moments in the two-dimension domain. It can be observed from Fig. 2(g)-(i) that the solution has more obvious periodicity in y. Irrespective of the spatial dimension of the domain, the solution is also bounded and tends to a steady state for the weak chemotaxis effect. This aligns with Theorem 2.3.

We now take $\chi = 10$ to represent that the chemotaxis effect is strong. The initial data is chosen as $(v_{10}, v_{20}, v_{30}) = (100, 10 + \varrho(x), 50 + \varrho(x))$, where $\varrho(x)$ is random noise uniformly distributed in $(-1, 1)$. The infection rates are selected as constant in the whole domain, where $\delta = 0.003$ and $\beta = 0.005$. The numerical results are displayed in Fig. 3. We introduce perturbations to the initial data of infected hosts and pathogens, but the solution still converges to a steady state in the one-dimension domain by Fig. 3(a)-(c). Additionally, the solution is bounded, in accordance with Theorem 2.4. For the two-dimension simulation, we find that infected hosts highly concentrate at certain positions when t is small and χ is large. When t exceeds 0.05, the solution appears to experience a numerical blow-up (synonymously referred to as finite-time blow-up), rendering it noncomputable within the desired tolerance. Biologically, this highly concentrated phenomenon before the blow-up is explained as spatial aggregation [22]. In fact, by virtue of Theorem 2.4 and Proposition

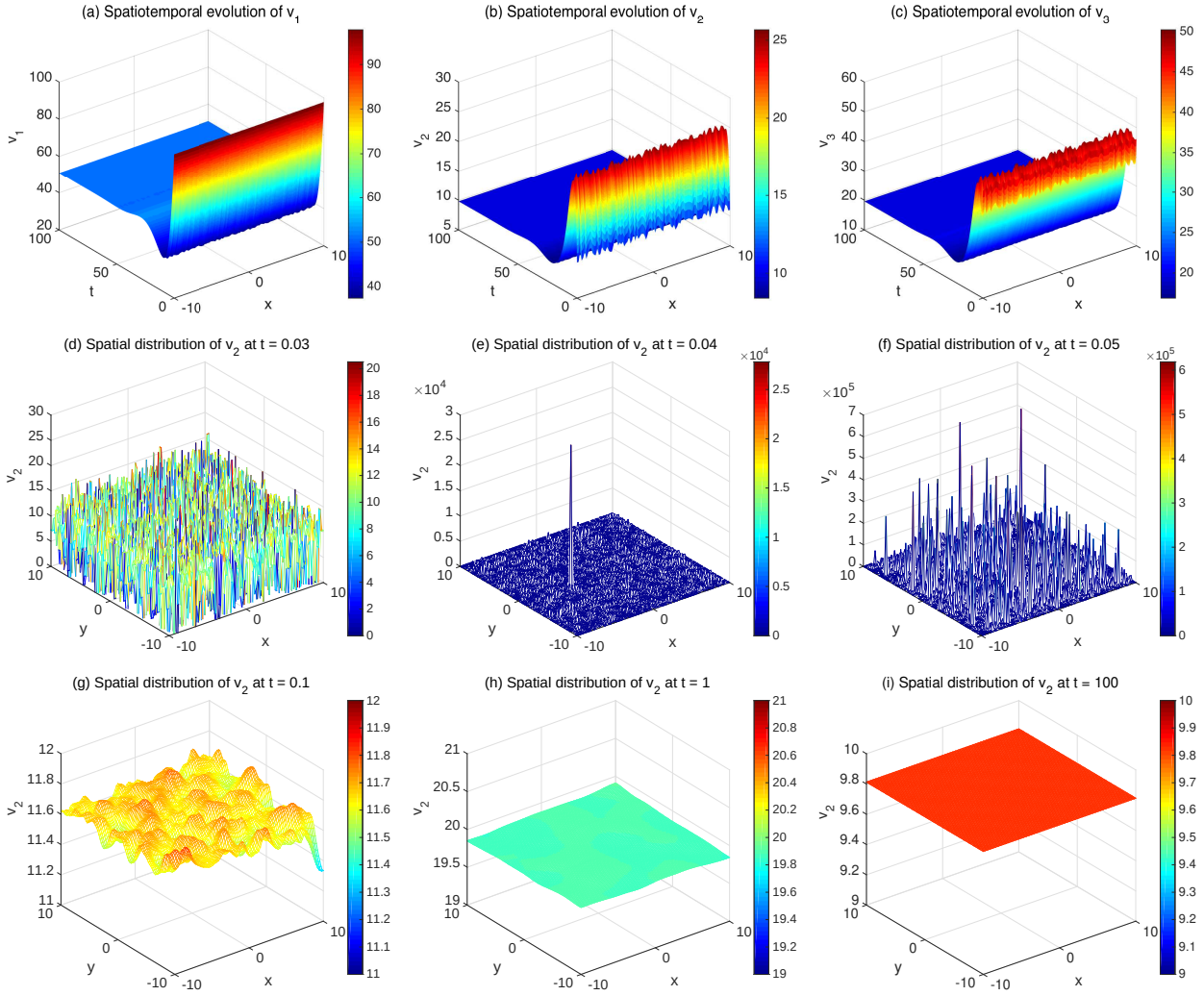

Fig. 3: $\chi = 10$ in model (1.2). (a)-(c): the spatiotemporal evolution of the solution for the one-dimensional domain. (d)-(f): the spatial distribution of v_2 at $t = 0.03, 0.04, 0.05$ for the two-dimensional domain, respectively. (g)-(i): the spatial distribution of v_2 at $t = 0.1, 1, 100$ after the regularisation of the chemotaxis.

3.1(i), we understand that the blow-up of the solution may occur for $\mathcal{R}_0 > 1$ and large χ in a two-dimensional domain. Mathematically, a standard approach to deal with this phenomenon is to introduce a regularisation term to (1.2). We shall use a density-dependent sensitivity regularisation, studied in [37–39]. Our new governing system becomes:

$$\begin{cases} \partial_t v_1 - d_1\Delta v_1 = (1+\varepsilon)\chi\nabla\cdot\left(\dfrac{v_1}{1+\varepsilon v_1}\nabla v_2\right) + \Lambda(x) - \mu v_1 - \dfrac{\delta(x)v_1v_2}{1+\sigma v_2} \\ \qquad\qquad - kv_1\ln\left(1+\dfrac{\beta(x)v_3}{k}\right), & x\in\Omega,\ t>0, \\ \partial_t v_2 - d_2\Delta v_2 = \dfrac{\delta(x)v_1v_2}{1+\sigma v_2} + kv_1\ln\left(1+\dfrac{\beta(x)v_3}{k}\right) - \theta v_2, & x\in\Omega,\ t>0, \\ \partial_t v_3 - d_3\Delta v_3 = \gamma v_2 - \alpha v_3, & x\in\Omega,\ t>0, \\ \nabla v_1\cdot\mathbf{n} = \nabla v_2\cdot\mathbf{n} = \nabla v_3\cdot\mathbf{n} = 0, & x\in\partial\Omega,\ t>0, \\ v_1(x,0) = v_{10}(x),\ v_2(x,0) = v_{20}(x),\ v_3(x,0) = v_{30}(x), & x\in\Omega. \end{cases} \tag{4.1}$$

According to [39], the notation of effective chemotaxis of model (4.1) is:

$$\bar{\chi} := \frac{1+\varepsilon}{1+\varepsilon v_1}\chi.$$

Note that $\bar{\chi}\to 0$ as $v_1\to\infty$. For large but bounded v_1, $\bar{\chi}\to\chi$ as $\varepsilon\to 0$. The effective chemotaxis in model (4.1) serves to maintain the boundedness of the solution. By the regularisation of the chemotaxis as (4.1), the numerical results are illustrated in Fig. 3(g)-(i), where ε is taken as 0.1. It is evident that the solution of the model remains bounded after the regularisation of the chemotaxis.

Nevertheless, further explanation is required to establish a connection between the blow-up of solutions and real-world process behavior, as blow-up phenomena are not observed in reality [18].

4.2 Spatial segregation

We apply the segregation indices introduced in [40] to measure the degree of segregation:

$$\eta(u,v) = \max_{x\in\bar{\Omega}}\{u-v\}\cdot\min_{x\in\bar{\Omega}}\{u-v\},$$

and

$$\kappa(u,v) = \frac{\|u-v\|_1}{\|u\|_1+\|v\|_1},$$

for $u(x), v(x) \in C(\bar{\Omega})$. Here, $\eta \in \mathbb{R}$ and $0 \leq \kappa \leq 1$. There is no segregation if $\eta \geq 0$ or $\kappa = 0$. If $\eta < 0$ and $\kappa > 0$, the segregation gets stronger as κ tends to one, while it gets worse as κ tends to zero. In this subsection, we always assume $\delta(x) = 0.3\cos x + 0.5$ and $\beta(x) = 0.5\cos x + 0.7$ in the one-dimensional domain $\Omega = (0, 2\pi)$. Clearly, the infection rate is the highest at positions $x = 0$ and 2π and the lowest at position $x = \pi$.

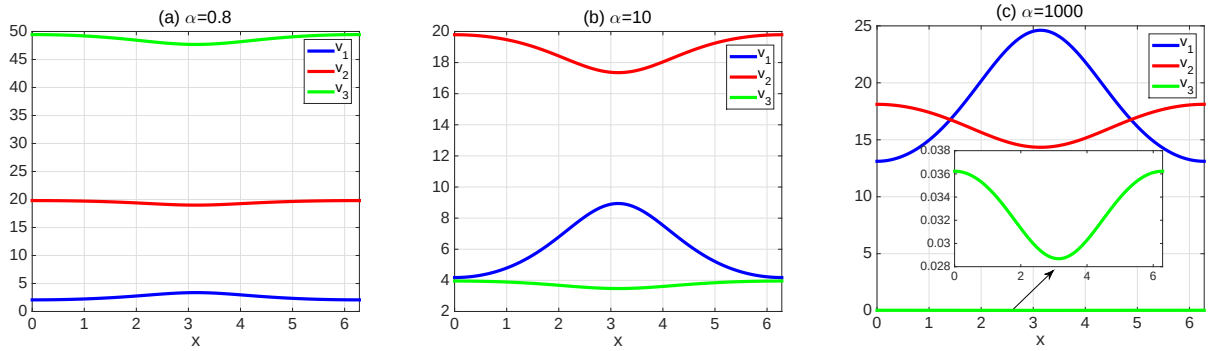

Fig. 4: The distribution of the steady states for model (1.2) with varying values of α when $\chi = 0.1$.

As assumed in model (1.2), susceptible hosts can only recognize infected hosts by the symptoms of infection, while they cannot recognize the pathogens because they are too small to detect. We choose $\chi = 0.1$ in Fig. 4, and the other parameter values are the same as those in the subsection 4.1 except for the death rate of pathogens in an external environment α. To better understand the segregation between susceptible and infected hosts, we give the distribution of the species according to α, which is illustrated in Fig. 4. The elevated mortality rate of pathogens is attributed to their difficulty in surviving independently of a host organism. It is noticeable that susceptible hosts are the highest at position $x = \pi$, where the infection rates are the lowest. It can also be observed that the concentration of pathogens decreases significantly with the increase of the mortality rate of pathogens, and eventually tends to zero as α approaches ∞. Correspondingly, the density of infected hosts decreases with the decrease of the concentration of pathogens.

Table 1: Segregation indices and infection fraction for different α.

α	$\eta(v_1, v_2)$	$\kappa(v_1, v_2)$	$\frac{\int_0^{2\pi} v_2 dx}{\int_0^{2\pi}(v_1+v_2)dx}$
0.8	277.0429	0.7650	0.8825
10	131.3565	0.5077	0.7539
1000	-51.3745	0.1409	0.4736

It follows from Table 1 that there is no discernible segregation between susceptible and infected hosts due to the positive values of η when the death rate of pathogens are 0.8 and 10, while the segregation phenomenon is observed when $\alpha = 1000$. This suggests that when pathogens cannot survive in an external environment for a long time, spatial segregation between susceptible and infected hosts can appear because newly infected hosts are mainly produced by the transmission of infected hosts. We find from Fig. 4(c) that the fraction of pathogens is rather small when $\alpha = 1000$, which is helpful to observe the segregation between susceptible and infected hosts. On the contrary, it is hard to segregate the hosts when the death rate of pathogens is small because the infection by pathogens can also increase the density of infected hosts to a large extent. Thus, there is much more significance by selecting a high death rate of pathogens to study the segregation phenomenon between susceptible and infected hosts.

We then turn to explore the effect of chemotaxis on the segregation between susceptible and infected hosts. In the following scenario, α is taken as 1000. Therefore, the infection caused by pathogens can be ignored. When there is no chemotaxis, the numerical result is given in Fig. 5(a). The parameter $\chi > 0$ demonstrates that susceptible hosts will move away from regions with a higher density of infected hosts. From Fig. 4(c) and Fig. 5(b), we can observe that the density of susceptible hosts decreases notably at positions $x = 0$ and 2π, but increases abruptly at position $x = \pi$ with the increase of the values of χ. In addition, the strong chemotaxis significantly contributes to the homogenization of the distribution of infected hosts and the heterogenization or dehomogenization of the distribution of susceptible hosts, which can be seen from Fig. 5(c).

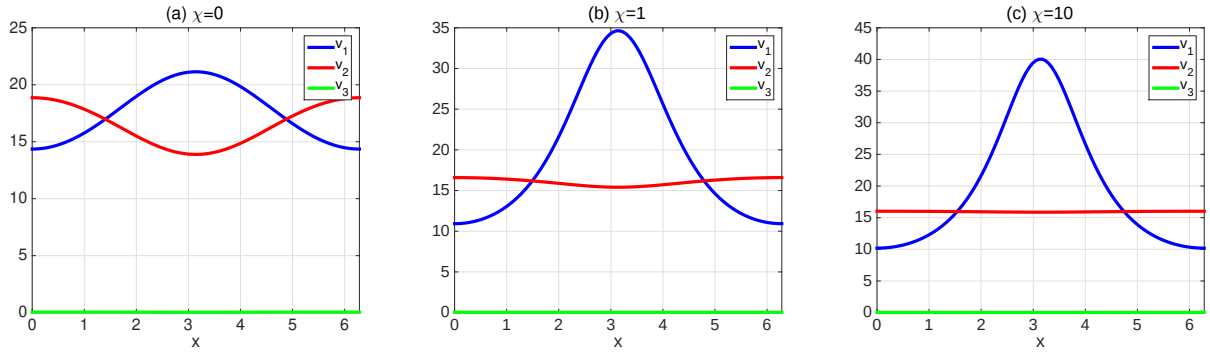

Fig. 5: The distribution of the steady states for model (1.2) with different values of χ when $\alpha = 1000$.

Table 2 reveals that there is segregation between susceptible and infected hosts due to the negative values of η. However, the segregation is weak because the values of κ are small and close to zero. Although the segregation gets better as χ increases, it has a limited impact on reducing the total infection number by comparing the infection fraction.

Table 2: Segregation indices and infection fraction for different χ.

χ	$\eta(v_1, v_2)$	$\kappa(v_1, v_2)$	$\frac{\int_0^{2\pi} v_2 dx}{\int_0^{2\pi}(v_1+v_2)dx}$
0	-32.6879	0.1114	0.4837
1	-108.8713	0.2039	0.4512
10	-140.9571	0.2284	0.4421

5 Discussion

In this work, we explored a reaction-chemotaxis-diffusion host-pathogen model including two distinct transmission processes, where we applied the saturated incidence to describe the disease transmission between hosts, and the negative binomial incidence to illustrate the infection by pathogens. The chemotactic response was employed to represent the directed movement of susceptible hosts either towards or away from already infected hosts. Nevertheless, susceptible hosts cannot move to or away from pathogens cognitively or directionally due to the undetectability of pathogen particles.

We have shown analytically the solvability of the model regarding the magnitude of χ. The model reduces to a reaction-diffusion model when χ is zero. Accordingly, the global existence of the solution and the existence of the global attractor in all dimensional domains were verified, contributing to the threshold dynamics in terms of the basic reproduction number. When χ is constrained within a narrow interval, we were also able to prove the global boundedness of the solution in any spatial dimension, while the bound of the solution depends on the initial data. When the constraint on χ is removed, we can only provide the boundedness of the solution in a one-dimensional domain. These theoretical findings enrich our comprehension of the dynamic properties of chemotactic host-pathogen models. We performed a series of numerical examples to explore the spatial aggregation and segregation caused by the chemotactic response. There is no spatial aggregation and the solution is always bounded when χ is zero or small in one- or two-dimensional domains according to Figs. 1 and 2. Similarly, the solution is also bounded in the one-dimensional domain when χ is large from Fig. 3. The numerical results are consistent with our theoretical results in Theorems 2.1-2.4. Nevertheless, when χ is large, it is found that the hosts take on aggregation phenomenon in the two-dimensional domain, and the solution blows up at finite time in the two-dimensional domain by Fig. 3. However, after the regularisation of the chemotaxis, the solution remains bounded. Whether the finite-time blow-up of solutions occurs for $n = 2$ mathematically is still an open question. In addition, the boundedness of the solution for arbitrary χ still requires further exploration for spatial dimension $n \geq 3$. We refer interested readers to [20], where some mathematical reasons for the occurrence of unbounded solutions for $n \geq 2$ were provided in a chemotaxis system. In the limiting scenario where σ approaches zero and k tends to infinity, we considered the chemotaxis-driven instability for the positive constant steady state when $\chi < 0$. Proposition 3.3 introduced three necessary conditions regarding the degree of the chemotaxis attraction for this scenario. For a more detailed exploration of Turing patterns, we recommend referring to [41] and the cited references therein.

We also studied whether the directed movement driven by the chemotaxis effect leads to spatial segregation. Our findings indicate that spatial segregation can appear if pathogens cannot survive in an external environment for a long time, while the strong repulsive chemo-

taxis among hosts alone does not effectively segregate susceptible and infected hosts, which is in obvious contrast to segregation observed in previous studies [40, 42]. This contrast can be attributed to two key factors. On one hand, the chemotaxis effect is not sufficiently suitable for describing the diffusion with cognition because we find that strong chemotactic repulsion can homogenize the distribution of infected hosts. On the other hand, there is only directed movement of susceptible hosts caused by the chemotactic repulsion of infected hosts, yet there is no corresponding directed movement of infected hosts. Consequently, it becomes challenging to spatially separate susceptible and infected hosts well. Therefore, the chemotaxis effect holds limited significance in reducing the total infection number. In future research, we will devote ourselves to developing host-pathogen models that incorporate enhanced cognitive diffusion mechanisms to explore the spatial structures driven by directed movement.

Acknowledgements

We would like to thank Yurij Salmaniw for his discussion and assistance in support of this work. The research of the second author was partially supported by the Natural Sciences and Engineering Research Council of Canada (Individual Discovery Grant RGPIN-2020-03911 and Discovery Accelerator Supplement Award PGPAS-2020-00090) and the Canada Research Chairs program (Tier 1 Canada Research Chair Award). The research of the third author was partially supported by the National Natural Science Foundation of China (No. 11571200) and the Natural Science Foundation of Shandong Province (No. ZR2021MA062).

Data Availability

Data sharing was not applicable to this article as no datasets were generated or analyzed during the current study.

References

[1] R.M. Anderson, R.M. May, Regulation and stability of host-parasite population interactions: I. Regulatory processes, J. Anim. Ecol., 47(1) (1978) 219-247.

[2] R.M. May, R.M. Anderson, Regulation and stability of host-parasite population interactions: II. Destabilizing processes, J. Anim. Ecol., 47(1) (1978) 249-267.

[3] R.M. Anderson, R.M. May, The population dynamics of microparasites and their invertebrate hosts, Philos. Trans. Roy. Soc. London Ser. B, 291(1054) (1981) 451-524.

[4] M. Begon, R.G. Bowers, N. Kadianakis, D.E. Hodgkinson, Disease and community structure: the importance of host self-regulation in a host-host-pathogen model, Amer. Nat., 139(6) (1992) 1131-1150.

[5] G. Dwyer, Density dependence and spatial structure in the dynamics of insect pathogens, Amer. Nat., 143(4) (1994) 533-562.

[6] B.T. Grenfell, A.P. Dobson, Ecology of Infectious Disease in Natural Populations, Cambridge University Press, Cambridge, 1995.

[7] J.V. Greenman, P.J. Hudson, Infected coexistence instability with and without density-dependent regulation, J. Theoret. Biol., 185(3) (1997) 345-356.

[8] Y. Wu, X. Zou, Dynamics and profiles of a diffusive host-pathogen system with distinct dispersal rates, J. Differential Equations, 264(8) (2018) 4989-5024.

[9] V. Capasso, G. Serio, A generalization of the Kermack-McKendrick deterministic epidemic model, Math. Biosci., 42(1-2) (1978) 43-61.

[10] O. Diekmann, J.A.P. Heesterbeek, Mathematical Epidemiology of Infectious Diseases: Model Building, Analysis and Interpretation, John Wiley and Sons, Chichester, 2000.

[11] H. McCallum, N. Barlow, J. Hone, How should pathogen transmission be modelled? Trends Ecol. Evol., 16(6) (2001) 295-300.

[12] C.J. Briggs, H.C.J. Godfray, The dynamics of insect-pathogen interactions in stage-structured populations, Amer. Nat., 145(6) (1995) 855-887.

[13] R.J. Knell, M. Begon, D.J. Thompson, Transmission dynamics of Bacillus thuringiensis infecting Plodia interpunctella: a test of the mass action assumption with an insect pathogen, Proc. Royal Soc. London Ser. B: Biol. Sci., 263(1366) (1996) 75-81.

[14] N.D. Barlow, Non-linear transmission and simple models for bovine tuberculosis, J. Anim. Ecol., 69(4) (2000) 703-713.

[15] E.F. Keller, L.A. Segel, Initiation of slime mold aggregation viewed as an instability, J. Theoret. Biol., 26(3) (1970) 399-415.

[16] Y. Tao, Z.-A. Wang, Competing effects of attraction vs. repulsion in chemotaxis, Math. Models Methods Appl. Sci., 23(01) (2013) 1-36.

[17] H. Li, R. Peng, F.B. Wang, Varying total population enhances disease persistence: qualitative analysis on a diffusive SIS epidemic model, J. Differential Equations, 262(2) (2017) 885-913.

[18] N. Bellomo, A. Bellouquid, Y. Tao, M. Winkler, Toward a mathematical theory of Keller-Segel models of pattern formation in biological tissues, Math. Models Methods Appl. Sci., 25(09) (2015) 1663-1763.

[19] Y. Tao, M. Winkler, Boundedness in a quasilinear parabolic-parabolic Keller-Segel system with subcritical sensitivity, J. Differential Equations, 252(1) (2012) 692-715.

[20] D. Horstmann, M. Winkler, Boundedness vs. blow-up in a chemotaxis system, J. Differential Equations, 215(1) (2005) 52-107.

[21] H. Li, R. Peng, T. Xiang, Dynamics and asymptotic profiles of endemic equilibrium for two frequency-dependent SIS epidemic models with cross-diffusion, European J. Appl. Math., 31(1) (2020) 26-56.

[22] N. Bellomo, K.J. Painter, Y. Tao, M. Winkler, Occurence vs. absence of taxis-driven instabilities in a May-Nowak model for virus infection, SIAM J. Appl. Math., 79 (5) (2019) 1990-2010.

[23] H. Li, T. Xiang, on a cross-diffusive SIS epidemic model with power-like nonlinear incidence, arXiv preprint arXiv: 2208.09571 (2022).

[24] N. Shigesada, K. Kawasaki, E. Teramoto, Spatial segregation of interacting species, J. Theoret. Biol., 79(1) (1979) 83-99.

[25] T.C. Schelling, Models of segregation, Amer. Econom. Rev., 59(2) (1969) 488-493.

[26] R.H. Martin, H.L. Smith, Abstract functional-differential equations and reaction-diffusion systems, Trans. Amer. Math. Soc., 321(1) (1990) 1-44.

[27] Y. Lou, X.-Q.Zhao, A reaction-diffusion malaria model with incubation period in the vector population, J. Math. Bio., 62(4) (2011) 543-568.

[28] A. Pazy, Semigroups of Linear Operators and Applications to Partial Differential Equations, Springer-Verlag, New York, 1983.

[29] J.K. Hale, Asymptotic Behavior of Dissipative Systems, American Mathematical Society, Providence, 1988.

[30] M. Winkler, Aggregation vs. global diffusive behavior in the higher-dimensional Keller-Segel

model, J. Differential Equations, 248(12) (2010) 2889-2905.

[31] L. Nirenberg, An extended interpolation inequality, Ann. Scuola Norm. Sup. Pisa., 20(4) (1996) 733-737.

[32] A. Friedman, Partial Differential Equations, Holt, Rinehart and Winston, New York, 1969.

[33] S. Ishida, K. Seki, T. Yokota, Boundedness in quasilinear Keller-Segel systems of parabolic-parabolic type on non-convex bounded domains, J. Differential Equations, 256(8) (2014) 2993-3010.

[34] W. Wang, X.-Q. Zhao, Basic reproduction numbers for reaction-diffusion epidemic models, SIAM J. Appl. Dyn. Sys., 11(4) (2012) 699-717.

[35] X.-Q. Zhao, Dynamical Systems in Population Biology, 2nd ed., Springer, New York, 2017.

[36] X. Ren, Y. Tian, L. Liu, X. Liu, A reaction-diffusion within-host HIV model with cell-to-cell transmission, J. Math. Biol., 76(7) (2018) 1831-1872.

[37] J.J.L. Velázquez, Point dynamics in a singular limit of the Keller-Segel model 1: Motion of the concentration regions, SIAM J. Appl. Math., 64(4) (2004) 1198-1223.

[38] J.J.L. Velázquez, Point dynamics in a singular limit of the Keller-Segel model 2: formation of the concentration regions, SIAM J. Appl. Math., 64(4) (2004) 1224-1248.

[39] O. Stancevic, C.N. Angstmann, J.M. Murray, B.I. Henry, Turing patterns from dynamics of early HIV infection, Bull. Math. Biol., 75 (2013) 774-795.

[40] H. Wang, K. Wang, Y.-J. Kim, Spatial segregation in reaction-diffusion epidemic models, SIAM J. Appl. Math., 82(5) (2022) 1680-1709.

[41] S. Pal, S. Ghorai, M. Banerjee, Analysis of a prey-predator model with non-local interaction in the prey population, Bull. Math. Biol., 80 (2018) 906-925.

[42] G. Liu, H. Wang, X. Zhang, Epidemic dynamics and spatial segregation driven by cognitive diffusion and nonlinear incidence, Stud. Appl. Math., 151 (2023) 643-675.